Ultraviolet radiation modelling using output from the chemistry climate model initiative

Kevin Lamy, Thierry Portafaix, Beatrice Josse, Colette Brogniez, Sophie Godin-Beekmann, Hassan Bencherif, Laura Revell, Hideharu Akiyoshi, Slimane Bekki, Michaela I. Hegglin, et al.

Atmos. Chem. Phys. Discuss., https://doi.org/10.5194/acp-2018-525
Manuscript under review for journal Atmos. Chem. Phys.
Discussion started: 11 June 2018

Atmospheric Chemistry and Physics Discussions

Ultraviolet Radiation modelling using output from the Chemistry Climate Model Initiative

Kévin Lamy[1], Thierry Portafaix[1], Béatrice Josse[2], Colette Brogniez[3], Sophie Godin-Beekmann[4], Hassan Bencherif[1,5], Laura Revell[6,7,8], Hideharu Akiyoshi[9], Slimane Bekki[4], Michaela I. Hegglin[10], Patrick Jöckel[11], Oliver Kirner[12], Virginie Marecal[2], Olaf Morgenstern[13], Andrea Stenke[6], Guang Zeng[13], N. Luke Abraham[14,15], Alexander T. Archibald[14], Neil Butchart[16], Martyn P. Chipperfield[17], Glauco Di Genova[18], Makoto Deushi[19], Sandip S. Dhomse[17], Rong-Ming Hu[4], Douglass Kinnison[20], Martine Michou[2], Fiona M. O'Connor[16], Luke D. Oman[21], Giovanni Pitari[18], David A. Plummer[22], John A. Pyle[14], Eugene Rozanov[6,23], David Saint-Martin[2], Kengo Sudo[24], Taichu Y. Tanaka[19], Daniele Visioni[18], and Kohei Yoshida[19]

[1]LACy, Laboratoire de l'Atmosphère et des Cyclones (UMR 8105 CNRS, Université de La Réunion, Météo-France), Saint-Denis de La Réunion, France
[2]Centre National de Recherches Météorologiques (CNRM) UMR 3589, Météo-France/CNRS, Toulouse, France
[3]Laboratoire d'Optique Atmosphérique (LOA), Université Lille 1 Sciences et Technologies, Villeneuve d'Ascq, France
[4]Laboratoire Atmosphères, Milieux, Observations Spatiales, Service d'Aéronomie (LATMOS), CNRS, Institut Pierre Simon Laplace, Pierre et Marie Curie University, Paris, France
[5]School of Chemistry and Physics, University of KwaZulu Natal, Durban, South Africa
[6]Institute for Atmospheric and Climate Science, ETH Zürich (ETHZ), Zürich, Switzerland
[7]Bodeker Scientific, Christchurch, New Zealand
[8]School of Physical and Chemical Sciences, University of Canterbury, Christchurch, New Zealand
[9]National Institute of Environmental Studies (NIES), Tsukuba, Japan
[10]Department of Meteorology, University of Reading, Reading, UK
[11]Institut für Physik der Atmosphäre, Deutsches Zentrum für Luft- und Raumfahrt (DLR), Oberpfaffenhofen, Germany
[12]Steinbuch Centre for Computing, Karlsruhe Institute of Technology, Karlsruhe, Germany
[13]National Institute of Water and Atmospheric Research (NIWA), Wellington, New Zealand
[14]Department of Chemistry, University of Cambridge, Cambridge, UK
[15]National Centre for Atmospheric Science, U.K.
[16]Met Office Hadley Centre (MOHC), Exeter, UK
[17]School of Earth and Environment, University of Leeds, Leeds, UK
[18]Department of Physical and Chemical Sciences, Universitá dell'Aquila, L'Aquila, Italy
[19]Meteorological Research Institute (MRI), Tsukuba, Japan
[20]National Center for Atmospheric Research (NCAR), Boulder, Colorado, USA
[21]National Aeronautics and Space Administration Goddard Space Flight Center (NASA GSFC), Greenbelt, Maryland, USA
[22]Environment and Climate Change Canada, Montréal, Canada
[23]Physikalisch-Meteorologisches Observatorium Davos World Radiation Centre, Davos Dorf, Switzerland
[24]Graduate School of Environmental Studies, Nagoya University, Nagoya, Japan

Correspondence to: K. Lamy (kevin.lamy@univ-reunion.fr)

Atmos. Chem. Phys. Discuss., https://doi.org/10.5194/acp-2018-525
Manuscript under review for journal Atmos. Chem. Phys.
Discussion started: 11 June 2018

Atmospheric Chemistry and Physics Discussions

Abstract.

We have derived values of the Ultraviolet Index (UVI) at solar noon from the Tropospheric Ultraviolet Model (TUV) driven by ozone, temperature and aerosol fields from the first phase of the Chemistry-Climate Model Initiative (CCMI-1). Since clouds remain one of the largest uncertainties in climate projections, we simulated only clear-sky UVI. We compared the UVI climatologies obtained from CCMI and TUV against present-day climatological values of UVI derived from satellite data (the OMI-Aura OMUVBd product) and ground-based measurements (from the NDACC network). Depending on the region, relative differences between the UVI obtained from CCMI and TUV and ground based measurements ranged between -4% and 11%.

We calculated the UVI evolution throughout the 21st century for the four Representative Concentration Pathways (RCPs 2.6, 4.5, 6.0 and 8.5). Compared to 1960s values, we found an average increase in UVI in 2100 (of 2-4%) in the tropical belt (30°N-30°S). For the mid-latitudes, we observed a 1.8 to 3.4 % increase in the Southern Hemisphere for RCP 2.6, 4.5 and 6.0, and found a 2.3% decrease in RCP 8.5. Higher UV indices are projected in the Northern Hemisphere except for RCP 8.5. At high latitudes, ozone recovery is well identified and induces a complete return of mean UVI levels to 1960 values for RCP 8.5 in the Southern Hemisphere. In the Northern Hemisphere, UVI levels in 2100 are higher by 0.5 to 5.5% for RCP 2.6, 4.5 and 6.0 and they are lower by 7.9% for RCP 8.5.

We analysed the impacts of greenhouse gases (GHGs) and ozone-depleting substances (ODSs) on UVI from 1960 by comparing CCMI sensitivity simulations (1960-2100) with fixed GHGs or ODSs at their respective 1960 levels. As expected with ODS fixed at their 1960 levels, there is no large decrease in ozone levels and consequently no sudden increase in UVI levels. With fixed GHG, we observed a delayed return of ozone to 1960 values, the same signal is observed on UVI, and looking at the UVI difference between 2090s values and 1960s values, we found an 8 % increase in the tropical belt during the summer of each hemisphere.

Finally we show that, while in the Southern Hemisphere UVI is mainly driven by total ozone column, in the Northern Hemisphere both total ozone column and aerosol optical depth drive UVI levels, with aerosol optical depth having twice as much influence on UVI as total column does.

Atmos. Chem. Phys. Discuss., https://doi.org/10.5194/acp-2018-525
Manuscript under review for journal Atmos. Chem. Phys.
Discussion started: 11 June 2018

Atmospheric Chemistry and Physics Discussions

1 Introduction

After the implementation of the Montreal Protocol, emissions of chlorine and bromine-containing ozone depleting substances (ODSs) have started to decrease and the ozone layer is showing signs of recovery (Morgenstern et al., 2008; Solomon et al., 2016). Nonetheless, greenhouse gas (GHG) emissions generally are still increasing and are expected to affect future ozone levels (Fleming et al., 2011; Revell et al., 2012). Global circulation model simulations project that the Brewer Dobson circulation will accelerate over the next century (Butchart, 2014), which would lead to a decrease of ozone levels in the tropics and an enhancement at higher latitudes (Hegglin and Shepherd, 2009). Ozone is one of the major factors affecting surface ultraviolet radiation (SUR). The levels of ultraviolet (UV) radiation on the surface are essential for life on earth. Overexposure to this radiation is the main cause of the development of non-melanoma and melanoma skin cancers. Non-melanoma skin cancer is induced by chronic exposure and melanoma is induced by repeated burning and chronic exposure (Matsumura and Ananthaswamy, 2004). Studies on human health and UV generally use the UV Index (UVI) (Mc Kinlay and Diffey, 1987) as a tool to quantify the impact of the UV radiation on the human skin. There is also a beneficial effect of UV radiation on human health through the synthesis of pre-vitamin D (Holick et al., 1980). UV radiation also impacts the biosphere (Erickson III et al., 2015) including the aquatic system, which plays a central part in biogeochemical cycles (Hader et al., 2007). Phytoplankton productivity is strongly affected by UV (Smith and Cullen, 1995), which can result in either positive or negative feedback on climate (Zepp et al., 2007).

The implementation of the Montreal Protocol on Subtances that Deplete the Ozone Layer, along with reductions in stratospheric chlorine and bromine alleviated increasing concerns about future surface UV radiation (Morgenstern et al., 2008). This protocol and its amendments drastically reduced the emissions of ODSs, i.e. the halocarbons. Nonetheless, recent studies on the evolution of ozone in a changing climate (Butchart, 2014) raised questions about future surface UV levels (Hegglin and Shepherd, 2009; Bais et al., 2011; Correa et al., 2013).

Numerous chemistry-climate model (CCM) simulations found an acceleration of the Brewer-Dobson circulation (BDC) (Butchart, 2014) due to the increase in atmospheric GHG concentrations. The BDC circulation was proposed by Brewer (1949) and Dobson (1956) to explain the latitudinal distribution of ozone and the amount of water vapor in the stratosphere. The BDC corresponds to a meridional transport in the stratosphere, with ascending air in the tropics and subsidence in the polar latitudes. The mechanism which drives this circulation is the dissipation of Rossby and gravity waves (Holton et al., 1995). Therefore, the strength of the BDC depends on the propagation and breaking of planetary waves. Rind et al. (1990) found that a doubling of carbon dioxide (CO_2) would lead to an increase in the residual-mean circulation due to the response from planetary waves, hence the residual-mean circulation (Andrews et al., 1987) can be seen as a proxy for the BDC. From the doubled CO_2 experiment, Rind et al. (2001) found a 30% increase of the troposphere to stratosphere mass exchange. Consequently, an accelerated loss of CFCs will reduce the timescale for ozone to recover (Shepherd, 2008). A strengthening of the BDC and an accelerated recovery of ozone will modify the distribution of ozone in the stratosphere and impact UV radiation at the surface.

While the ozone layer in the stratosphere absorbs UV radiation, it is not the only factor affecting surface levels of UV. The distance between the Sun and Earth is responsible for about $\approx 7\%$ of the UV variability on the ground (Frederick et al., 1989).

Atmos. Chem. Phys. Discuss., https://doi.org/10.5194/acp-2018-525
Manuscript under review for journal Atmos. Chem. Phys.
Discussion started: 11 June 2018

The 11-year solar cycle accounts for about 6% of the UV variability in the stratosphere (Gray et al., 2010). Solar zenith angle (SZA) plays a key role for the intensity of surface UV radiation. For higher SZA the path travelled through the atmosphere is longer, hence absorption and diffusion increase and the UV response to changes in total ozone column (TOZ) is affected (Brühl and Crutzen, 1989). Clouds and aerosols also cause variability (Bais et al., 1993). In most cases, clouds attenuate the UV signal on the surface by about 15 to 45% (Calbó et al., 2005). Broken cloud cover can also enhance the surface UV (Mayer et al., 1998). Krzyścin and Puchalski (1998) found a 1.5% increase in UV erythemal for a 10% decrease of aerosol optical depth (AOD) and up to a 30% decreases of UV erythemal can be observed due to biomass burning emissions (Lamy et al., 2018). In the UVA region, a mean reduction of irradiance of 15.2% per unit of AOD slant column has been observed by Kazadzis et al. (2009). Nitrogen dioxide and sulphur dioxide have also a small effect on UV irradiance (Solomon et al., 1999; Vaida et al., 2003).

In the context of a changing climate and with the use of stratospheric CCM simulations, Hegglin and Shepherd (2009) found a 3.8% increase of UVI in the tropics between 2090s and 1960s. In the Northern Hemisphere, they found a 9% decrease in UVI due to increased transport of ozone. As part of the precursor multi-model activity to CCMI, CCMVal-2, Bais et al. (2011) also calculated UVI evolution between 1960 and 2100 and reported a small increment in the tropics of 0.9%, a 7.5% and 9.8% decrease in northern and southern high latitudes and a 4.1% decrease in mid latitudes. In both of these studies the largest UV reduction was found in Antarctica. This is consistent with the recovery of the ozone layer.

Following from these studies, we investigate the evolution of surface UV radiation using the latest simulations from the first phase of the Chemistry-Climate Model Initiative (CCMI-1), a project initiated by Future Earth's IGAC (International Global Atmospheric Chemistry) and the World Climate Research Programme's SPARC(Stratosphere-troposphere Processes and their Role in Climate) as a succesor to the continuity of the Chemistry-Climate Model Validation Activity (CCMVal) and Atmospheric Chemistry and Climate Model Intercomparison Project (ACCMIP) (Eyring et al., 2013). We use CCMI data and the Tropospheric Ultraviolet Model (TUV) (Madronich et al., 1998) to calculate surface irradiance over the globe.

In Section 2, we will explain the methodology used to calculate ground surface irradiance from CCMI data and TUV, and describe the TUV model. We will briefly present the CCMI models along with the different experiments performed for CCMI. A validation of UVI, calculated with CCMI data and TUV, against satellite and ground-based measurements will be presented in Section 3. A discussion of the spread between CCMI models and on the resulting sensitivity of TUV will be conducted in Section 3. In Section 4, we examine the possible evolution of UVI at different latitudinal bands following the representative concentration pathways (RCPs) Meinshausen et al. (2011)). We also analyze the difference between monthly values of UVI in the 1960s and 2090s. Sensitivity simulations using concentrations of ODSs and GHGs fixed at constant 1960 levels were also performed for the CCMI exercise. These allow us to assess the impact of GHGs and ODSs on UVI individually. An analysis of the impact of AOD on UVI is presented in Section 4.4. The last section will discuss and conclude the findings of the present study.

Atmos. Chem. Phys. Discuss., https://doi.org/10.5194/acp-2018-525
Manuscript under review for journal Atmos. Chem. Phys.
Discussion started: 11 June 2018

2 Data and methodology

2.1 Ultraviolet Modeling

UV irradiance at the Earth's surface is calculated with the TUV radiative transfer model (version 5.3) for the entire globe on a 2° by 2° grid. The spectral solar irradiance simulated at the Earth's surface range from 280 to 450 nm with a 1 nm resolution. The spectral irradiance is then integrated to obtain the UVI (Mc Kinlay and Diffey, 1987). The required input for the UV calculation are:

- Total Ozone Column (TOZ)
- Total Nitrogen Dioxide (TNO_2)
- Ozone Profile (OP)
- Temperature Profile (TP)
- Aerosol Optical Depth (AOD)
- Aerosol Ångström exponent (α)
- Single Scattering Albedo (SSA)
- Ground Surface Albedo (ALB)
- Altitude (z)

As input for TUV we used data from the latest CCMI simulations (Hegglin and Lamarque, 2015). A brief description of the CTMs or CCMs used in this study is provided in Table 1 and Table 2, while more details are available in Morgenstern et al. (2017). From these models the monthly output from the refC2, senC2rcp26, senC2rcp45, senC2rcp85, senC2fODS and senC2fGHG simulations were retrieved. RefC2 is a transient "future reference" simulation covering the period 1960-2100 with a 10 year spin-up which starts in 1950. The aim of this simulation is to investigate the future evolution of the atmosphere. From 1960 to 2005 concentrations are prescribed from observations. After 2005, projections of GHGs from the RCP 6.0 scenario are used (Masui et al., 2011). The RCPs are scenarios used to study future Earth's climate.They are composed of four pathways representative of the GHG concentrations along the 21st century which lead to a radiative forcing of 2.6, 4.5, 6.0 or 8.5 $W.m^{-2}$ in 2100. While RCP 2.6 suppose strong effort to reduce GHG emissions. RCP 8.5 is based on large GHG emissions, CH_4 concentrations is particularly high in this scenario compared to others.

ODS concentrations are prescribed according to the A1 scenario for halogens (WMO, 2011). senC2rcp26, senC2rcp45 and senC2rcp85 are similar to refC2 but instead of following RCP 6.0 for GHGs, they follow RCP 2.6, 4.5 and 8.5 (Meinshausen et al., 2011) respectively. The senC2fODS and senC2fGHG simulations are similar to refC2 but with ODSs or GHGs fixed at their respective 1960 levels. The senC2 simulations were optional for the intercomparison exercise. Therefore only a few

Atmos. Chem. Phys. Discuss., https://doi.org/10.5194/acp-2018-525
Manuscript under review for journal Atmos. Chem. Phys.
Discussion started: 11 June 2018

models provided results for both senC2fGHG and senC2fODS experiments (Table 2). A complete description of all CCMI-1 simulations is given by Eyring et al. (2013) and Morgenstern et al. (2017).

From these CCMI simulations, we used the following monthly global fields to calculate UVI: total ozone column (TOZ), vertical distribution of ozone (OP) and temperature (TP), ground surface albedo (ALB) and altitude or pressure. For TNO_2 we vertically integrated the volume mixing ratio of NO_2. As single scattering albedo (SSA) was not available , we choose here to use the latest global aerosol monthly climatology from Kinne et al. (2013) as input for the TUV model. We used the median AOD and the Ångström exponent (440-870 nm) from three models which provided this variable; CHASER MIROC-ESM, MRI-ESM1r1 and GEOSCCM. Due to the lack of reliable data, total column sulphur-dioxide (TSO_2) was set to zero. nonetheless TSO2 could be an important factor of UVI variability (Zerefos et al., 1986).

Radiative transfer modelling in cloudy conditions is still a challenging task. Bais et al. (2011) used cloud modification factor along with UV irradiance projections in order to simulate future UV changes due to clouds. Here, our focus is on the UV evolution for distinct RCP scenarios and on the influence of GHGs and ODSs. In addition, clouds and aerosols remain the main sources of uncertainties in climate projections (IPCC, 2013), and the accuracy of UV modelling depends strongly on the accuracy of the input parameters. For these reasons, we choose here to analyze only clear-sky conditions. There is also the uncertainty on the absolute mean value of the extra-terrestriel solar UV spectrum used at the top of the atmosphere in TUV. Differences between proposed solar UV spectra can reach 5% (Meftah et al., 2016). In the present study, we use (Gorshelev et al., 2014; Serdyuchenko et al., 2014) solar spectrum.

The horizontal and vertical grids vary between the CCMI models. All of the required CCMI data are therefore interpolated to a 2° by 2° grid with 86 pressure levels, the highest pressure level is at 0.001 hPa. There were 18 models participating in the CCMI simulations. It was thus not possible to perform the same number of UV projections for the entire 21st century due to computational limitations. The error associated with this simplification on the UV projections is discussed in Section 4.1. A few other simplifications were made to reduce computational time. OP and TP are averaged zonally but still vary through the 21st century. For each CCMI monthly output, we simulated UV irradiance at local solar noon and for the 15th of each month.

2.2 UVI modelling cases.

As stated above, we used four RCP scenarios and two sensitivity simulations, but not all models provided these specific runs (Table 2). To ensure that the resulting TUV simulations would be directly comparable with each other. We defined two experiments from two sets of models, these are summarized in Table 2. The first set is composed of models which provided the refC2, senC2rcp26, senC2rcp45 and senC2rcp85 simulations (see Table 2). From this set of models, we can study the impact on UVI from different RCP scenarios (experiment 1, EXP1). Each model in this set provided simulations which cover 2000-2100 at minimum. The second set is composed of models which provided refC2, senC2fODS and senC2fGHG simulations. This set allows us to investigate the impact of fixing GHGs or ODSs on UV irradiance from 1960 to 2100 (experiment 2, EXP2). We also designed a third experiment (EXP3), based on the models used in EXP1. We performed three simulations; the first one with transient TOZ and AOD (hereafter EXP3A), a second with TOZ fixed at its 2000s decadal mean value and transient AOD (EXP3FTOZ), and the last one with AOD fixed at present-days climatological values (Kinne et al., 2013) and transient TOZ

Atmos. Chem. Phys. Discuss., https://doi.org/10.5194/acp-2018-525
Manuscript under review for journal Atmos. Chem. Phys.
Discussion started: 11 June 2018

Atmospheric Chemistry and Physics Discussions

(EXP3FAOD). For experiments we calculated the mean and median of the various input parameters of the different selected models, such as ozone, temperature or ground albedo, and used it as input for the radiative transfer model to obtain UVI_{MEAN} and UVI_{MEDIAN}.

3 Model Validation: present-days values

3.1 Model Validation

In this section, we first investigate the usage of CCMI model data as input for the TUV radiative transfer model. The results are compared against present-day climatological values of UV irradiance obtained from ground-based and satellite measurements. According to Koepke et al. (1998), the UVI modelling error is about 5 % for a coverage factor of 2 standard deviation.

We gathered UVI data spanning at least the period 2000 to 2017 for six stations representing six latitudinal bands. The various stations and their characteristics are presented in Table 3. They are all part of the Network for the Detection of Atmospheric Composition Change (NDACC) (De Mazière et al., 2018). UV measurements at these stations are made by a spectroradiometer. Just like UVI obtained by the model, UVI is obtained from the spectral irradiance. These types of measurements has an uncertainty of about 5%. All of these stations began measuring UV in the early 2000s, except for Reunion Island where observations started in 2009. In order to compare the ground-based measurements to our modelling results, we filter cloudy conditions with the clear-sky flag provided with each station's measurements. We also select data with a SZA as close as possible to the SZA at local noon, with no more than 2.5° difference. From this we derive a monthly climatology for the 2005-2017 period (UVI_{GB}). From the closest grid point of the UVI_{MEAN} and UVI_{MEDIAN} simulation, we derive the same UVI monthly climatology. We do this only for the refC2 simulation.

We also derive a climatology for each station from the OMI OMUVBd product (Krotkov et al., 2002) which is represented by the orange curve in Figure 1 and it will be called hereafter UVI_{OMI}. OMUVBd is a level-3 daily global gridded UV-B irradiance product derived from the Ozone Monitoring Instrument (OMI), which is a nadir-viewing spectrometer. Measurements started in 2004. The instrument covers the spectral region 264-504 nm. The algorithm used to compute surface spectral UV irradiance is the TOMS Surface UV-B flux algorithm (Tanskanen et al., 2007). OMUVBd has previously been evaluated against ground based stations. Tanskanen et al. (2007) found a median overestimation of 0 to 10% of the erythemal doses calculated by OMI. Jégou et al. (2011) found a 12.8 ± 3.6 % mean relative difference between OMI clear-sky UV measurements and ground-based measurements made at the SIRTA observatory (Palaiseau, France) in 2008 and 2009. Brogniez et al. (2016) also analysed this product against three ground-based stations located at Villeneuve d'Ascq and the Observatoire de Haute-Provence, both in France, and at Saint-Denis in Reunion island. They observed a systematic overestimation of UVI at solar noon. Once more we select UVI only at local solar noon, which is provided in the OMUVBbd product. In order to be as close as possible to our simulation and since OMUVBDd has sometimes missing values over the ground based stations at the 15th of each month, we also select 10 days per month centred around the 15th of each month. The results are presented in Figure 1.

For every station, the UVI_{MEAN} (red curve) and UVI_{MEDIAN} (green curve) are close to the observed climatological UVI (black curve) with the individual model (light blue curves) spreading around the observations. UVI_{OMI} tends to be a lightly

higher than the observations. We also calculate the mean absolute and relative difference between these monthly climatological UVI and ground-based observations. Table 3 summarizes these statistics. Here, a similar conclusion can be drawn, except for the Palmer station, where UVI_{MEAN} and UVI_{MEDIAN} are always closer to ground-based observations than UVI_{OMI}. UVI_{OMI} tends to overestimate UVI by 6.8% at Lauder, and up to 29.3% at Barrow. While the relative difference is large at high latitude stations, the absolute difference in UVI is small. For instance, the 10.5 % relative difference in UVI_{MEAN} at the Palmer station, translates into an absolute difference of about 0.33 UVI units. In the tropics, at Mauna Loa, a relative difference of 5.40% is equivalent to a similar absolute difference of UVI (0.29 UVI units). We have to be careful when we interpret UVI at high latitude stations, as the magnitude of UVI is quite small most of the time due to large solar zenith angles. Nonetheless, at low and mid-latitudes the UVI differences observed are fully compatible with the errors attached with the measurements and models (Koepke et al., 1998).

For short time scales of about 10 years, a part of the TOZ variability observed at ground-based stations is due to the wind variability above the station (Poulain et al., 2016). In the refC2 runs, models produce their own wind and temperature fields.In a separate simulation which we do not analyze here, the refC1SD simulation, the model is forced by boundary conditions obtained from reanalyses (Eyring et al., 2013). Unlike refC1SD, refC2 simulations are not designed to reproduce the interannual variability and trends in stratospheric dynamics and hence ozone which are observed over individual stations between 2000-2010. Differences between observed and simulated dynamical variability is possibly a significant source of the discrepancies between observed and modelled UVI, but it is difficult to estimate. The differences in the dynamics of the models certainly contribute to the spread in the model results. Altough by using refC1SD, better agreement may be expected for the validation of CCMI models, the main objective of this study is to study the UVI evolution during the 21st century, which is not possible using refC1SD simulation; therefore we choose to only validate the result from the refC2 simulations.

Simulated UVI has also been compared to UVI_{OMI} satellite measurements. Boxplots summaries of the relative differences between each model and UVI_{OMI} are represented in Figure 2. Over the globe, UVI_{MEAN} and UVI_{MEDIAN} deviate from OMUVBd observations by respectively -16.8 $\pm$ 12.9 % and -17.3 $\pm$ 12.5 %. The response is quite different amongst the individual models. While the closest mean relative difference is observed for the MOCAGE model, it is also the one with the highest variability. In all cases, CCMI models are lower than UVI_{OMI}. As stated before previous studies on UVI_{OMI} validation against ground-based spectral measurements found a systematic overestimation. Therefore, in the present study, it is coherent to find lower values of simulated UVI compared to the UVI_{OMI}.

As a last test, we took the TOZ fields from the 18 models which performed a refC2 simulation from 2000 to 2010 and used them as input for TUV. From there we obtained 18 UVI fields covering the same period and calculated the median, hereafter UVI_{ALLM}.

The global relative difference between these two data sets is presented in Fig. 3. This result allows us to assess the sensitivity of the radiative transfer model to different ozone inputs. Between both UVI fields there is a mean relative difference of 0.19 $\pm$ 1.9 %. Around the globe, the differences range from -2% up to 2%. Conclusively, we can say that averaging CCMI TOZ fields prior to using them as input for TUV induce only a small difference in the resulting average UVI.

Atmos. Chem. Phys. Discuss., https://doi.org/10.5194/acp-2018-525
Manuscript under review for journal Atmos. Chem. Phys.
Discussion started: 11 June 2018

Atmospheric Chemistry and Physics Discussions

Due to computational constraints, it was not possible to compute UVI for each scenario and for all models throughout the 21st century. UVI_{MEDIAN} and UVI_{MEAN} compare well to the ground-based observations (Figure 1) and have the lowest dispersion among the different models (Figure 2). We therefore calculate the UVI from the different simulations based on median input fields derived from the available models, rather than the single model fields in order to save computational time and show only UVI_{MEDIAN} in the next section.

4 UV Projection throughout the 21st century

In the following subsection (4.1), we will discuss the evolution of UVI and TOZ over the 21st century for six latitudinal bands and for the four RCP scenarios by analysing the results of EXP1. We will then (section 4.2) look at the zonal monthly difference n UVI and TOZ between the 2000s and 2090s. In Section 4.3 we evaluate the impact of GHGs and ODSs on the evolution of UVI and TOZ in EXP2. Again, we will start by looking at the percent change of UVI and TOZ from 1960 to 2100. We then investigate the differences between the 1960s and 2090s.

4.1 Temporal evolution of UVI during the 21st century according to different RCPs

To investigate the evolution of UVI and TOZ throughout the 21st century, we choose the following latitudinal bands. Southern and northern high latitudes are defined from 90° to 60° S and 60° to 90° N, respectively. Southern and northern mid-latitudes are defined from 60° to 30° S and 30° to 60° N, respectively. Finally, southern and northern tropical latitudes are defined from 30° to 0° S and 0° to 30° N, respectively. We then calculate the zonal mean percent change in the 2090s compared with the 1960s. This was done for the four RCP scenarios. Results are presented in Figure 4. Relative percent changes between the 1960s and 2090s are summarised in Table 4 for all latitudinal bands. In order to compare our results to previous studies we also reported results from Bais et al. (2011) and Hegglin and Shepherd (2009).

Figure 4 shows, as expected, that negative changes in UVI are usually correlated with positive changes in TOZ, and vice versa, except in the northern mid and tropical latitudes where both TOZ and AOD drives UVI variability at the end of the 21st century (section 4.4). In the southern polar region (Fig 4f), we observe the well known decrease of TOZ due to ODS. The ozone layer starts to recover around 2000. Between 2000 and 2100 there is a 10 % increase of TOZ for RCP 2.6 and a 16% increase for RCP 8.5. Consequently, there is a significant decrease of UVI, between 16 to 26 % for these scenarios between 2000 and 2100. Generally, the higher the radiative forcing, the more pronounced is the TOZ increase and UVI decrease. Compared to the 1960s, UVI will still be higher in 2100 by approximately 6.7%, 5.7% and 3.9% for RCP 2.6, 4.5 and 6.0, respectively. Only RCP 8.5 allows a complete return of UVI values in this region. Most of the UVI variability should in theory be explained by the recovery of the ozone layer; which we will verify in Section 4.4. The same behaviour is observed in the northern high latitudes, however, the magnitude is weaker. Compared to 1960s values, UVI will be 5.5%, 1.7% and 0.5% higher for RCP 2.6, 4.5 and 6.0 respectively. For RCP 8.5, there is a strong decrease of UVI (7.9%).

The same observation is made for the southern mid-latitudes with a maximal increase of TOZ of $\sim 9\%$ along with a maximum decrease of UVI of $\sim 12\%$ (Fig 4d) between 2000 and 2100. Compared to 1960 values, UVI percent changes in 2100 are

Atmos. Chem. Phys. Discuss., https://doi.org/10.5194/acp-2018-525
Manuscript under review for journal Atmos. Chem. Phys.
Discussion started: 11 June 2018

Atmospheric Chemistry and Physics Discussions

within 0 and 3% depending on the RCP scenarios. In 2100 for RCP 2.6, while TOZ is slightly lower than its 1960 values ($\sim$ 1%), UVI is higher by $\sim$ 3%. Again, the maximum change occur for the strongest radiative forcing increase (RCP 8.5). Here, GHG effects are stronger, and consequently there is more ozone in this region and UV is weaker compared to 1960 values. In the Northern Hemisphere, while TOZ does not vary more than 1% between 1960 and 2000, we observe a significant growth between 2000 and 2100, $\sim 8\%$ for RCP 8.5. As expected UVI percent changes appear to be anticorrelated with TOZ percent changes between 2000 and 2050, but after 2050 while TOZ still increases, UVI is almost constant. A similar situation can be observed in the northern tropical band, where TOZ appears to change not more than 1% between 2000 and 2100, however we observe a 2% to 4% increase in UVI during this period. The largest UVI percent change is observed for the lowest change of radiative forcing (RCP 2.6) (Fig 4a). At the northern mid- and tropical latitudes TOZ is not the principal driver of UVI changes (Section 4.4). For the southern tropics, TOZ and UVI are well anti-correlated, changes during the 21st century are very small and are confined within 0-3% for the period 2000 to 2100 (Fig 4b). Nonetheless, in this region, at the end of the 21st century, UVI will still be about 3% higher compared with in the 1960s. In the tropics, we observe a decreasing UVI from 2000 to 2050, then UVI increases from 2050 to 2100.

RCP 8.5 presents either negative changes or lowest increase of UVI, it is also correlated with increase of TOZ. Methane emissions are large in RCP 8.5 and (Morgenstern et al., 2018) found that TOZ increase with increasing methane in CCMI models.

A similar study was carried out by Bais et al. (2011) within the CCMVal-2 activity, Bais et al. (2011) used the refB2 experiment which used the SRES A1B scenario for GHGs (a scenario close to RCP 6.0). Annual-mean surface UVI percent changes were computed against the 1975-1984 mean. Between 1975 and 2100 they observe a 7.48% and 9.80% UVI percent change decrease in the northern and southern high latitudes respectively. Here, between 1960 and 2100, we only observed a similar decrease ($\sim$ 7.9%) in northern high latitudes for RCP 8.5. For the other scenarios, in this region, we find UVI percent changes between 0.5 to 5.5%. In the southern high latitudes, UVI values are higher than the 1960 baseline for RCP 2.6, 4.5 and 6.0 by 6.7%, 5.7% and 3.9% respectively. For RCP 8.5, there is complete return of UVI to its 1960 values. In the southern mid-latitudes, while Bais et al. (2011) also noted a decrease of UVI (4.16%) during the 21st century, we find UVI increases by 3.4, 2.6, 1.8 % for RCP 2.6, 4.5, 6.0, respectively. For RCP 8.5, we found a 2.3% decrease in UVI. And, while Bais et al. (2011) found a decrease in the Northern Hemisphere for these latitudes, here we show that UVI increases in all scenarios except RCP 8.5. In the tropical belt (30° North to 30° South), between 2000 and 2100, Bais et al. (2011) found changes of UVI of about 1%. We found similar results with smaller values, between 0 to 3%.

Hegglin and Shepherd (2009) conducted a study on UVI changes due to stratospheric circulation-driven changes in the ozone distribution. They used the Canadian Middle Atmosphere Model (CMAM) simulation performed for the CCMVal intercomparison. By comparing UVI between 1960-1970 and 2090-2100, they observed an evolution at all latitudes close to the one found by Bais et al. (2011). Likewise they found an increase of UVI in the tropics of about 4%. This was also shown by Butler et al. (2016). To conclude, the CCMVal-2 results from Bais et al. (2011), Hegglin and Shepherd (2009) and our results show similar conclusions for the UVI evolution in the tropics, but our results are different in the northern tropical and mid-latitudes depending on the RCP scenario. As stated before, UVI is influenced mainly by TOZ but also by AOD, ALB, TNO2, OP and

TP. Hegglin and Shepherd (2009) used the analytical formula by Madronich (2007) to determine UVI, which only takes into account relative changes in TOZ. Bais et al. (2011) used a radiative transfer calculations, but aerosol properties were fixed to present climatological values. This could explain the different conclusion obtained in the present study for the Northern Hemisphere. To better understand the evolution of UVI in the northern mid and tropical latitudes, we will look at these other parameters in section 4.4.

We looked here at the evolution of UVI throughout the 21st century. In the next section, we will quantify in more detail the difference between the 2000s and the 2090s and between different climate scenarios.

4.2 Global UVI levels at the end of the 21st century.

UVI and TOZ zonal monthly differences between the 2000s and 2090s are presented in Fig. 5, for four RCPs for both UVI (left column) and TOZ (right column). There is some missing values during the winter months, because we chose a threshold for the SZA of less than 60 °to calculate the UVI.

First, we note that the strongest mean relative difference (MRD) of UVI or TOZ over the globe is associated with the strongest radiative forcing change. For RCP 8.5, UVI MRD over the globe is -7.9% and TOZ MRD is 6.74%. For RCP 2.6 we calculate a UVI MRD of -1.4 % and a TOZ MRD of 2.1%.

During the months of September, October and November and in each RCP, there is a strong decrease of UVI (more than 24%) associated with a strong increase of TOZ in the southern polar region between July and up to November. This is due to the strong recovery of the ozone layer in this region.

We calculate a decline of UVI in southern mid-latitudes associated with a rise in TOZ for all scenarios. In northern mid-latitudes, while TOZ levels increase with increasing radiative forcing, we do not observe a corresponding decrease of the UVI. This is due to decreasing AOD (Section 4.4).

The zero line separating a decrease of UVI at high latitudes from an increase at low latitudes appears to shift towards the equator as the radiative forcing increases. Thus the regions where UVI increases (up to 4 to 6 %) are concentrated around the equator with the increase in radiative forcing related to GHG concentrations. This could be explained by the larger GHG concentrations in the RCPs with higher radiative forcing, which are expected to play an important role for the BDC circulation (Butchart, 2014).

In the following sections we will investigate the impact of GHG, ODS and AOD on the UVI separately.

4.3 Effects of greenhouse gases and ozone depleting substances on future UVI.

The role of GHG and ODS on UVI variability from 1960 to 2100 is investigated in this section. To investigate the effects of GHGs and ODSs on UVI variability between 1960-2100, we analysed the CCMI sensitivity experiments senC2fGHG and senC2fODS These are simulations based on refC2 (RCP 6.0), but with fixed GHG and ODS at constant 1960 concentrations, respectively. The CCMI models used in this part are those which provided data from refC2, senC2fGHG and senC2fODS. For the previous experiment (EXP1), we used the median AOD provided by three CCMI models (CHASER-MIROC-ESM, GEOSCCM and MRI) as input for the radiative transfer model. Here, we fixed AOD by taking the climatological values

provided by Kinne et al. (2013). The UVI and TOZ evolution for these two sensitivity experiments and refC2 are presented in Fig. 6.

As expected TOZ shows the smallest trends in the simulations with fixed ODS; the same conclusion can be drawn for UVI. Since the senC2fGHG and refC2 simulations are in close agreement in the Antarctic region, climate change has the smallest influence on TOZ variation (Dhomse et al., 2018) and therefore on UVI variation in this region.

From these two experiments, we note that the return of TOZ to 1960 levels will be later following the fixed GHG scenario, at northern and southern high latitudes (Fig. 6e,f).

In the southern mid-latitudes (Fig 6d), a similar behaviour appears, the TOZ and UVI percent changes increase or decrease more rapidly with transient GHG concentrations. This is comparable in the Northern Hemisphere (Fig 6c), where GHGs induce a rapid increase of TOZ and a rapid decrease of UVI which are expected to reach $\sim$ 3% and $\sim$ -3% in 2100, respectively.

In the tropics (Fig 6a,b), ODS accounts for about 2% of UVI and TOZ variability. Variations in GHG concentrations appear to have almost no effect on UVI and TOZ until the middle of the 21st century. There is a 2% increase of UVI, which appears around 2070. This can be observed for the fixed GHG and fixed ODS simulations. The percent change in UVI for the refC2 simulation stabilizes around 2070. In this region, GHGs are responsible for the acceleration of the BDC which induces an decrease of ozone in the lower stratosphere. But they are also responsible for the cooling in the upper stratosphere which induces an increase of ozone. Therefore, the small magnitude of changes in this region could be explained by the compensating GHGs effects in the simulations (Kirner et al., 2015; Morgenstern et al., 2018).

Global monthly relative differences between the 2090s and 1960s are also plotted in Figure 7 for both, UVI (left column), and TOZ (right column) for the refC2, senC2fODS and senC2fGHG simulations.

With fixed ODS, there is a 3.75% mean relative difference of UVI over the globe driven by increasing GHGs which have affect the circulation. In the tropical belt changes are $\sim$ 2% higher compared to the standard refC2 run especially in the summer for both hemispheres. Nonetheless, the tropical region is also the place where UVI has the highest absolute values, therefore even a small relative increase means a decent increase of absolute values. With fixed GHG, the effects of ODSs are minimal for the difference between 2100 and 1960.

4.4 Others effects affecting UVI.

In Sections 4.1 and 4.2, we found UVI increases in the northern mid and tropical latitudes, which were not correlated with TOZ changes. In Figure 8, we present the percent change of UVI, TOZ, and AOD in the northern high, mid and low latitudes for the EXP3A, EXP3FTOZ and EXP3FAOD experiments. This is also done for the southern latitudes (Figure 9). In Table 5, we summarize the UVI percent changes between 2100 and 2000 for three EXP3 experiments. We also report the TOZ and AOD changes.

At the mid-latitudes in EXP3FAOD, UVI decreases and is clearly anticorrelated with TOZ changes (blue curve, Fig.8b). For the same region in EXP3FTOZ, there is a 6% UVI percent change in this region in 2100 (green curve, Fig.8b). On the same figure, in EXP3A, UVI (orange curve) also increases by a smaller amount (up to $\sim$ 4% at the end of the 21st century). Both TOZ and AOD drive the UVI variability in this region. As the RCPs project a decline in aerosols precursor emissions (van

Vuuren et al., 2011), AOD decreases especially in the Northern Hemisphere and thus has strong effect on UVI. It is the same situation at the northern tropics (Fig. 8c,f and i), where AOD decreases by $\sim$ 16% and TOZ only changes slightly (<1%). The experiments with transient AOD and either fixed or varible TOZ exhibit almost the same percent change in UVI. This would indicate that AOD changes drive the UVI at these latitudes where TOZ variations are small. At northern high latitudes, AOD decreases by $\sim$ 80% and TOZ increases by $\sim$ 4% at the end of the century. With transient AOD and TOZ, UVI decreases by $\sim$ 3% (orange curve, Fig. 8a) and appears to follows the TOZ variability along the 21st century. In this region both TOZ and AOD drive UVI levels. For a medium decrease of AOD and very small changes of TOZ, AOD appears to be the main driver of UVI levels in the tropics.

In the Southern Hemisphere, the situation is different, as shown in Fig. 9. UVI percent changes are driven by the TOZ percent changes, which are important due to the recovery of the ozone layer. In addition AOD percent changes are very small in this region. In the southern high, mid and tropical latitudes, where there are small AOD percent changes compared to northern middle and tropical latitudes, UVI variability is driven by TOZ changes. The simulations with transient TOZ and either fixed AOD (blue curve) or transient AOD (orange curve) are almost identical and there is almost no UVI change if TOZ is fixed (green curve).

In summary, the UVI evolution observed in the Northern Hemisphere (Section 4.1) can be explained by both TOZ and AOD changes (Figure 8). In the Southern Hemisphere TOZ is still the main driver of UVI variability.

This last result shows that UVI evolution in the future will not only depends on TOZ but also on AOD. However AOD remains, besides clouds, one of the biggest sources of uncertainties in climate projections (IPCC, 2013). Additionaly, single scattering albedo (SSA),which was fixed at present-day climatoligcal values, has a strong effect on AOD absorption of UVI (Correa et al., 2013). Future studies should be conducted taking into account the impacts of clouds, AOD and SSA on future UVI levels.

5 Conclusions

We have shown that the use of CCMI model data with a radiative transfer model (TUV) enable current climatological values of UVI to be reproduced. Satellite UVI observations show a constant positive bias compared to ground-based observations (Tanskanen et al., 2007; Brogniez et al., 2016). UVI simulated with CCMI model data over the globe presents a negative median relative difference compared to satellite observations ranging between 0 to 20%. UVI simulated with CCMI model data presents a mean relative difference ranges from -4% to 11% compared to ground-based observations. In comparison to ground-based observations, we reproduce the monthly climatological variability at six stations spread across latitudes.

We investigated the impact of ODS and GHG on UVI. We confirm the role of GHGs in accelerating the return of UVI to 1960 levels via accelerating the ozone recovery. GHGs accounts for approximately 3.8% of the UVI changes between 1960 and 2100. While ODS have an effect on UVI between 1960 to 2050 due to ozone depletion, fixed GHG simulation show small changes of UVI.

Atmos. Chem. Phys. Discuss., https://doi.org/10.5194/acp-2018-525
Manuscript under review for journal Atmos. Chem. Phys.
Discussion started: 11 June 2018

Atmospheric Chemistry and Physics Discussions

In the context of a changing climate, surface UV irradiance is projected globally over the 21st century. We investigate here the changes for different RCP scenarios (Fig 4). In all scenarios at high southern latitudes, as TOZ return to 1960 levels, UVI is expected to return to 1960s values. It has already been found that ozone returns dates will arrive sooner should GHG emissions follow RCP 8.5 (Dhomse et al., 2018; WMO, 2014). We find here that UVI levels are mainly driven by TOZ changes at these latitudes, therefore UVI will also return to 1960 levels sooner for RCP 8.5.

In mid-latitudes, TOZ should increase in both hemispheres for all RCPs except RCP 8.5. The higher emissions of GHG assumed in RCP 8.5 cause significant differences between RCP 8.5 and the other scenarios. In the Southern Hemisphere, UVI levels are driven by TOZ, but in the Northern Hemisphere, the declining AOD from the median of three CCMI models oppose the effect of a TOZ increase. AOD and TOZ are drivers of UVI variability in this hemisphere with AOD being approximately twice as important as TOZ. Further studies are needed to investigate this issue thoroughly. In our present work, only AOD and the Ängström exponent are evolving through the 21st century, and SSA was fixed to present-day climatological values. Higher values of SSA would increase the absorption effectiveness of AOD and thus impact UV radiation (Correa et al., 2013). Regionally varying SSA changes are expected globally (Takemura, 2012). The upcoming Aerosol and Chemistry Intercomparison Project (AerChemMIP) (Collins et al., 2017) will provide an opportunity to examine this subject.

Zonal mean UVI variability is limited to 0-3% over the tropics. This result is similar to those found by Bais et al. (2011) and Hegglin and Shepherd (2009). Logically the increases are higher in the summer of both hemisphere; where local maxima of 8 to 10% were found. An increase of 10% in the tropics is a matter of concern, as the tropics is already the region with the highest values of UVI, therefore even a small percent increase could have strong effect on the biosphere. The impact of these types of increase on human health, the biosphere and consequently on biogeochemical cycles should be the subject of future studies.

Atmos. Chem. Phys. Discuss., https://doi.org/10.5194/acp-2018-525
Manuscript under review for journal Atmos. Chem. Phys.
Discussion started: 11 June 2018

Atmospheric Chemistry and Physics Discussions

Model	Institution	PIs	References
ACCESS-CCM	U. Melboune, AAD, NIWA	K. Stone, R. Schofield, A. Klelociuk, D.Karoly, O. Morgenstern	Morgenstern et al. (2009), Stone et al. (2016)
CCSRNIES MIROC3.2	NIES, Tsukuba, Japan	H. Akiyoshi, Y. Yamashita	Imai et al. (2013), Akiyoshi et al. (2016)
CHASER (MIROC-ESM)	U. Nagoya, JAMSTEC, NIES	K. Sudo, T. Nagashima	Sudo et al. (2002), Sekiya and Sudo (2012), Watanabe et al. (2011)
CMAM	CCCma, Canada	D. Plummer, J. Scinocca	Jonsson et al. (2004), Scinocca et al. (2008)
CNRM-CM5-3	CNRM, Toulouse, France	M. Michou, D. Saint-Martin	Michou et al. (2011), Voldoire et al. (2013)
EMAC-L90	DLR, Oberpfaffenhofen, Germany	P. Jöckel, H. Tost, A. Pozzer, M. Kunze, O. Kirner,	Jöckel et al. (2010), Jöckel et al. (2016)
GEOSCCM	NASA GSFC, Greenbelt, USA	L. D. Oman, S. E. Strahan	Molod et al. (2015), Oman et al. (2011)
HadGEM3-ES	MOHC, UK	F. M. O'Connor, N. Butchart, S. C. Hardiman, S. T. Rumbold	Hardiman et al. (2017), Walters et al. (2014), O'Connor et al. (2014), Madec et al. (2015), Hunke et al. (2010)
LMDZrepro	LMD, IPSL, Paris, France	S. Bekki, M. Marchand, F. Lott, D. Cugnet, L. Guez, F. Lefevre, S. Szopa, R.M Hu	Dufresne et al. (2013), Marchand et al. (2012), Szopa et al. (2013)
MOCAGE	CNRM, Toulouse, France	B. Josse,V. Marecal	Josse et al. (2004), Guth et al. (2016)
MRI-ESM1r1	MRI JMA, Tsukuba, Japan	M. Deushi, T. Y. Tanaka, K. Yoshida	Yukimoto et al. (2012), Deushi and Shibata (2011)
NIWA-UKCA	NIWA, Wellington, NZ	O. Morgenstern, G. Zeng	Morgenstern et al. (2009), Morgenstern et al. (2017)
SOCOL	PMOD/WRC, IAC/ETHZ	E. Rozanov, A. Stenke, L. Revell	Revell et al. (2015), Stenke et al. (2013)
ULAQ	U. L'Aquila, Italy	G. Pitari, G. Di Genova, D. Visioni	Pitari et al. (2014)
UMSLIMCAT	U. Leeds, UK	S. Dhomse, M. P. Chipperfield	Tian and Chipperfield (2005)
UMUKCA	U. Cambridge, UK	N. L. Abraham, A. T. Archibald, R. Currie, J. A. Pyle	Morgenstern et al. (2009), Bednarz et al. (2016)
WACCM (CESM1)	NCAR	D. Kinisson, R. R. Garcia, A. K. Smith, A. Gettelman, D. Marsh, C. Bardeen, M. Mills	Marsh et al. (2013), Solomon et al. (2015), Garcia et al. (2017)

Table 1. CCMI Model with Principal Investigator (PIs) and institutions.

Atmos. Chem. Phys. Discuss., https://doi.org/10.5194/acp-2018-525
Manuscript under review for journal Atmos. Chem. Phys.
Discussion started: 11 June 2018

Atmospheric Chemistry and Physics Discussions

Characteristics	EXP1	EXP2	EXP3		
			EXP3A	EXP3FTOZ	EXP3FAOD
Simulation	refC2 (RCP 6.0) RCP 2.6 RCP 4.5 RCP 8.5	refC2 (RCP 6.0) senC2fODS senC2fGHG	refC2 (RCP 6.0)		
TOZ	Transient	Transient	Transient	Fixed (2000-2010 values)	Transient
AOD	Transient	Fixed (Kinne et al., 2013)	Transient	Transient	Fixed (Kinne et al., 2013)
MultiModelMedian from	CCSRNIES MIROC3.2 CMAM LMDZrepro SOCOL ULAQ	ACCESS-CCM CCSRNIES MIROC 3.2 CHASER (MIROC-ESM) CMAM LMDZrepro NIWA-UKCA UMSLIMCAT WACCM	same as EXP1		

Table 2. Characteristics of the experiment conducted in this study.

Station	Latitude	Longitude	Relative Difference [%]			Absolute Difference		
			MEAN	MEDIAN	OMI	MEAN	MEDIAN	OMI
Mauna Loa	19.54° N	155.58° W	5.4	4.4	16.0	0.3	0.2	1.1
Saint-Denis	20.09° S	55.5° W	-3.5	-5.3	13.6	-0.3	-0.5	1.5
Villeneuve d'Asqc	50.61° N	3.14° E	2.5	2.8	24.5	0.2	0.01	0.8
Lauder	45.04° S	169.68° E	-3.9	-5.9	6.9	-0.2	-0.4	0.3
Barrow	71.32° N	156.68° W	2.9	2.0	29.3	0.04	0.02	0.6
Palmer	64.77° S	64.05° W	10.6	10.3	8.1	0.3	0.3	0.2

Table 3. Mean UVI relative and absolute difference of the monthly climatology between UVI_{MEAN}, UVI_{MEDIAN}, UVI_{OMI} to the ground-based measurements (UVI_{GB}).

If we define the UVI from ground-based measurements as UVI_{GB}, the differences are calculated as:

Relative Difference is defined as: $RD = 100\frac{UVI_{MEAN} - UVI_{GB}}{UVI_{GB}}$.

Absolute Difference is defined as: $RD = UVI_{MEAN} - UVI_{GB}$.

The same calculation applies to UVI_{MEDIAN} and UVI_{OMI}. For Barrow and Palmer station we selected the six months of their respective summer.

Atmos. Chem. Phys. Discuss., https://doi.org/10.5194/acp-2018-525
Manuscript under review for journal Atmos. Chem. Phys.
Discussion started: 11 June 2018

Atmospheric Chemistry and Physics Discussions

Region	RCP				RCP 6.0 with fixed AOD	senC2fODS	senc2fGHG	Bais et al. (2011)	Hegglin and Shepherd (2009)
	2.6	4.5	6.0	8.5					
60°- 90 °N	5.5	1.7	0.5	-7.9	-4.8	-0.6	1.4	-7.48	-9.1
30°- 60 °N	8.3	5.2	5.0	-1.4	-1.9	2.3	0.7	-4.10	-3.6
0°- 30 °N	2.8	2.7	2.7	0.9	2.9	6.5	0.1	0.89	3.8
0°- 30 °S	2.6	2.9	2.9	1.5	3.0	6.6	0.5		
30°- 60 °S	3.4	2.6	1.8	-2.28	0.3	3.7	1.7	-4.16	0.
60°- 90 °S	6.7	5.7	3.9	0.	-2	-0.1	2.7	-9.8	3.2

Table 4. Percent changes in UVI between 2100 and 1960.

Results for RCP 2.6, 4.5, 6.0 and 8.5 are obtained from EXP1 experiment.

Results for RCP 6.0 with fixed AOD, senC2fODS and senC2fGHG are obtained from EXP2 experiment.

Region	UVI			TOZ	AOD	Comments
	EXP3A	EXP3FTOZ	EXP3FAOD			
90 - 60 N	-2.1	2.1	-5.5	4.5	-78	TOZ and AOD drive UVI levels
30 - 60 N	3.8	6.2	-2.8	3.0	-77	TOZ and AOD drive UVI levels
0 - 30 N	3.5	2.3	1.2	-0.5	-15	TOZ and AOD drive UVI levels
0 - 30 S	0.6	0.0	0.5	0.2	-0.3	TOZ drives UVI levels
30 - 60 S	-6.1	0.1	-6.0	5.6	-4.16	TOZ drives UVI levels
60 - 90 S	-26.8	-3.2	-26.7	11.8	-1.5	TOZ drives UVI levels

Table 5. Percent Changes in UVI, TOZ and AOD between 2100 and 2000 for the EXP3A, EXP3FTOZ and EXP3FAOD experiments.

Atmos. Chem. Phys. Discuss., https://doi.org/10.5194/acp-2018-525
Manuscript under review for journal Atmos. Chem. Phys.
Discussion started: 11 June 2018

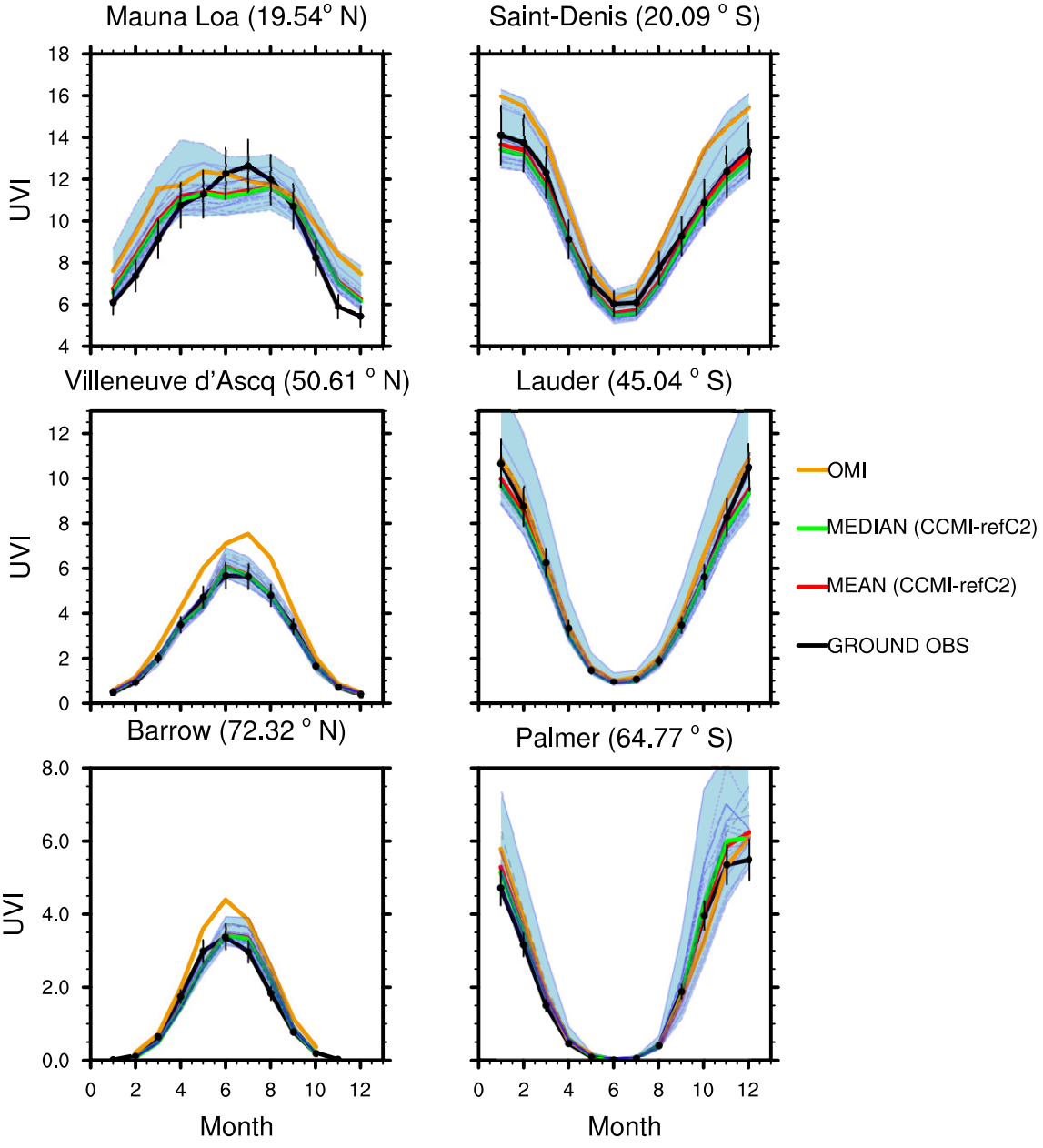

Figure 1. UVI_{GB} (2000-2010) for six NDACC stations along with the respective closest grid point from CCMI&TUV UVI simulation (UVI_{MEAN} and UVI_{MEDIAN}). Station measurements are represented in the black curve with a 2σ dispersion bar. UVI_{MEAN} and UVI_{MEDIAN} are represented in green and red. Each CCMI models are represented in light blue, the shaded blue area represents the spread of the models. UVI_{OMI} from the OMUVBd product are in orange.

Atmos. Chem. Phys. Discuss., https://doi.org/10.5194/acp-2018-525
Manuscript under review for journal Atmos. Chem. Phys.
Discussion started: 11 June 2018

Atmospheric Chemistry and Physics Discussions

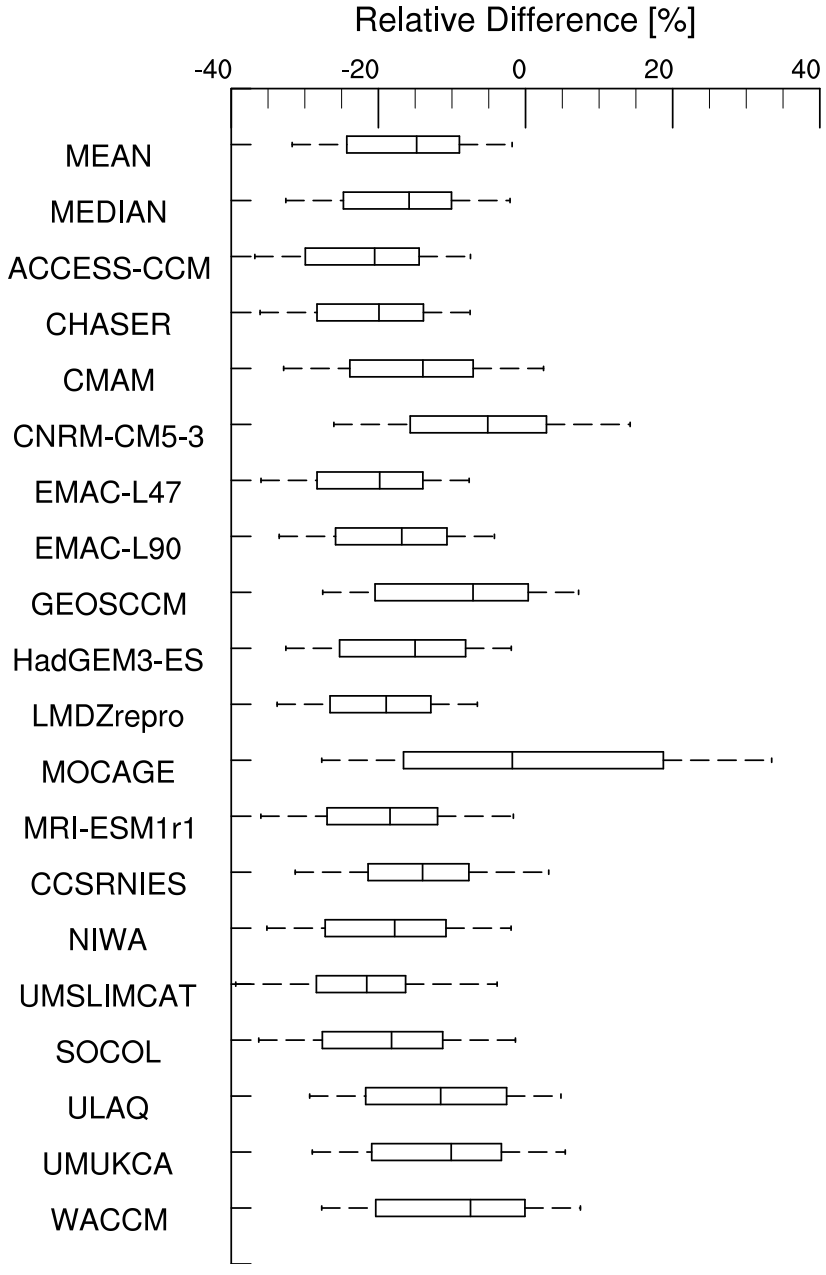

Figure 2. Boxplots summaries of the relative differences between the monthly UVI from CCMI models (refC2) and the monthly mean OMUVBd product for the period 2000-2010. Left and right end of the box are the first and third quartile respectively. The line inside the box is the median or second quartile. Left and right end of the whiskers are the mean $\pm$ 1-standard deviation.

For a model M, (M being Mean, Median, ACCESS-CCM, CHASER, ...) from which we obtained $\mathrm{UVI_M}$, we compute: $\mathrm{UVI_{RD}}[\%] = 100\frac{UVI_{\mathrm{M}}-UVI_{\mathrm{OMI}}}{UVI_{\mathrm{OMI}}}$

Atmos. Chem. Phys. Discuss., https://doi.org/10.5194/acp-2018-525
Manuscript under review for journal Atmos. Chem. Phys.
Discussion started: 11 June 2018

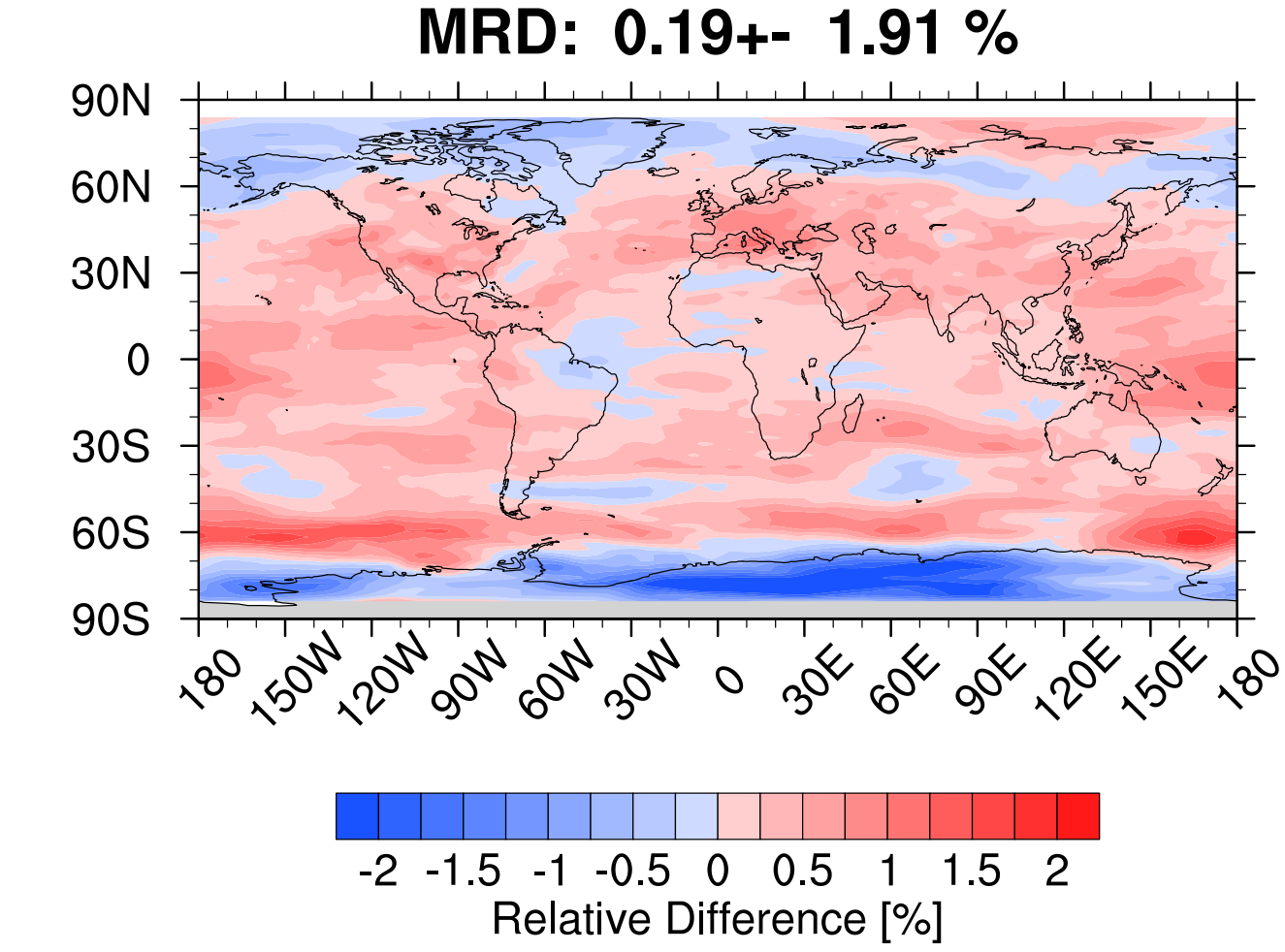

Figure 3. UVI annual mean relative difference between the median UVI obtained from the 18 CCMI model data used and TUV and the UVI obtained from the CCMI median TOZ used with TUV for the period 2000-2010.

$\mathrm{UVI_{RD}}[\%] = 200\frac{UVI_{\mathrm{ALLM}} - UVI_{\mathrm{MEDIAN}}}{UVI_{\mathrm{ALLM}} + UVI_{\mathrm{MEDIAN}}}$

Atmos. Chem. Phys. Discuss., https://doi.org/10.5194/acp-2018-525
Manuscript under review for journal Atmos. Chem. Phys.
Discussion started: 11 June 2018

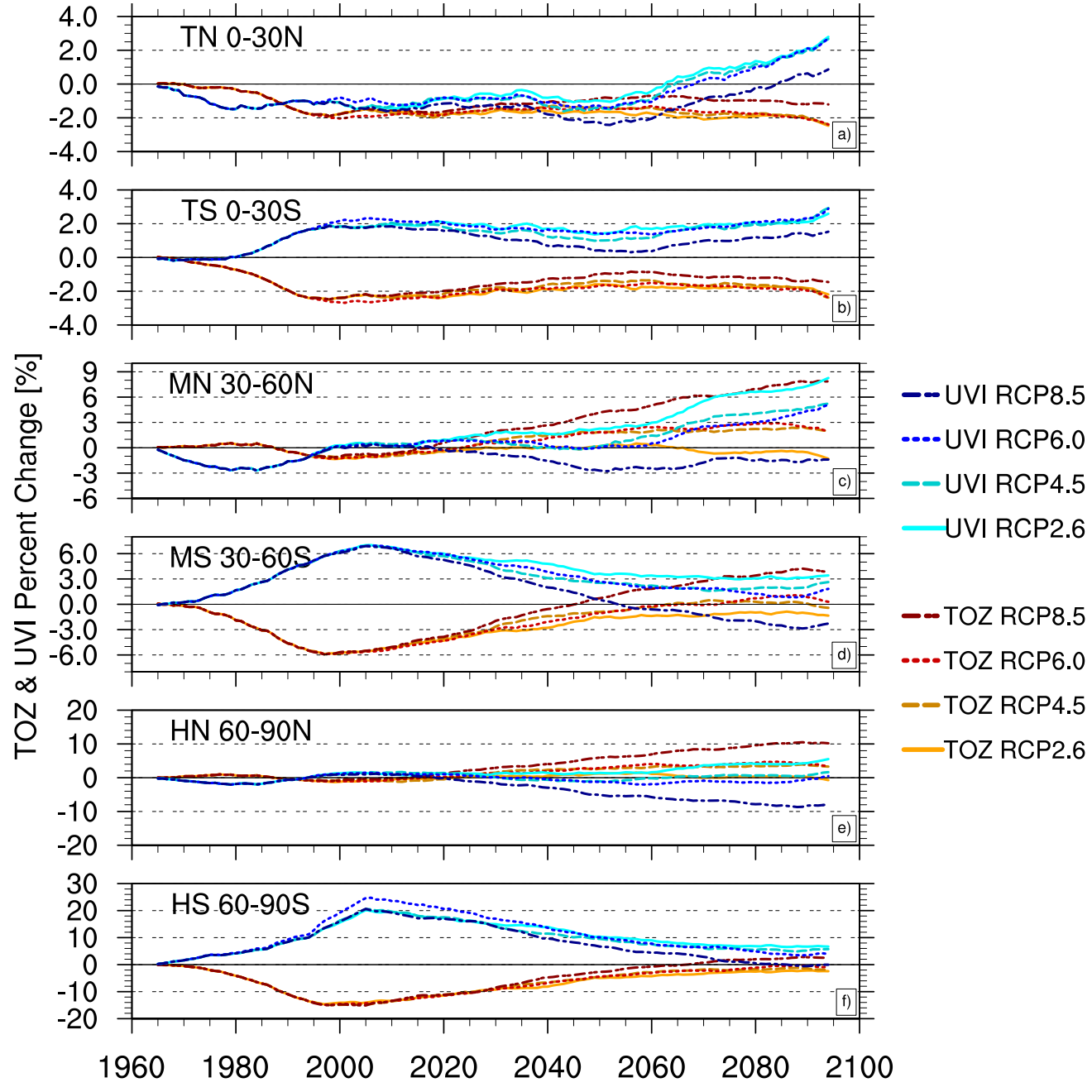

Figure 4. UVI and TOZ percent change relative to 1960-2070 values for six latitudinal bands; Northern Tropical band (0°- 30 °N), Southern Tropical band (0°- 30 °S), Northern Mid Latitude band (30°- 60 °N), Southern Mid Latitude band (30°- 60 °S), Northern High Latitude band (60°- 90 °N), Southern High Latitude band (60°- 90 °S). UVI changes are represented in different shades of blue for the four RCPs scenarios. TOZ changes are represented in different shades of red.

Atmos. Chem. Phys. Discuss., https://doi.org/10.5194/acp-2018-525
Manuscript under review for journal Atmos. Chem. Phys.
Discussion started: 11 June 2018

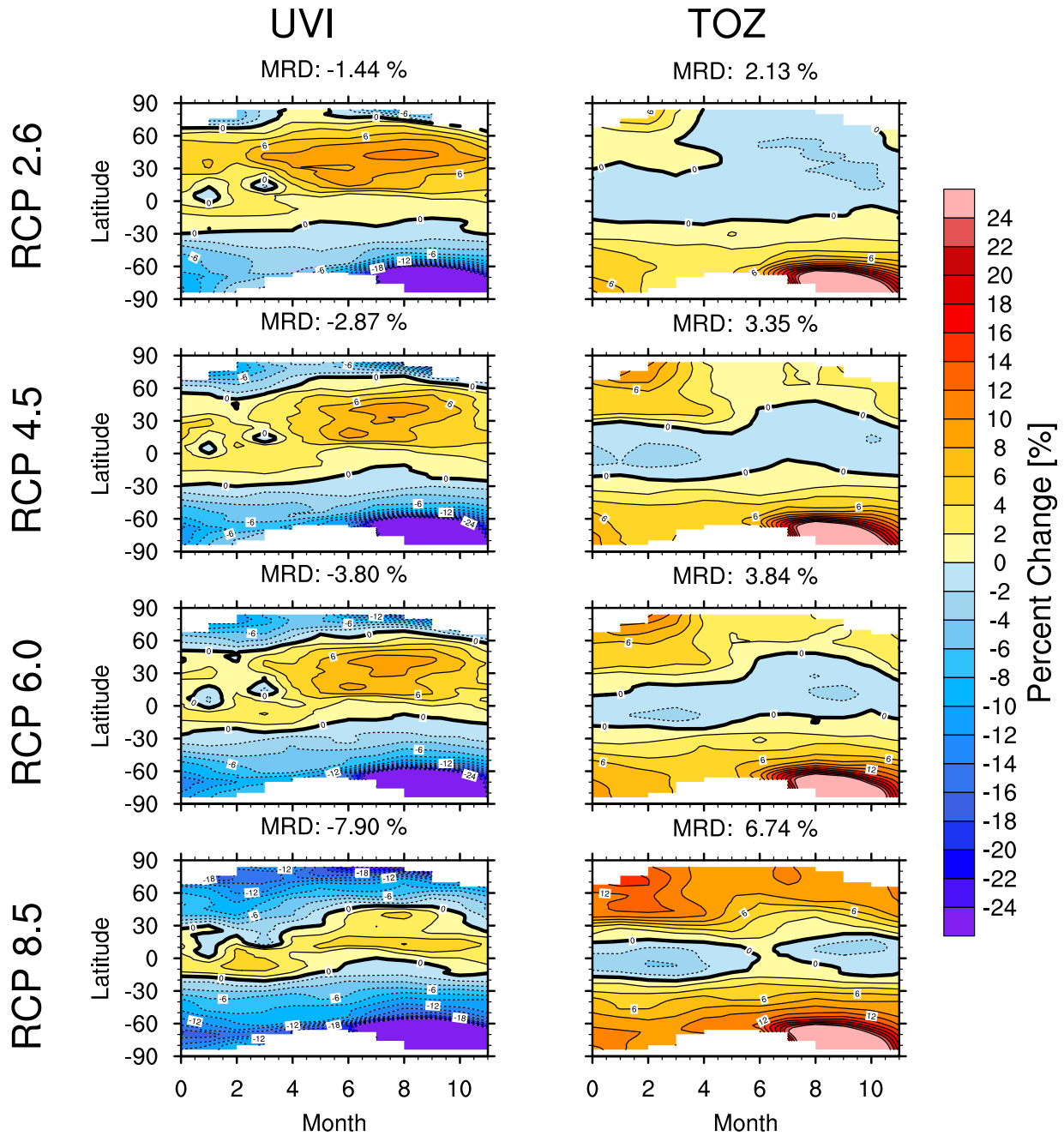

Figure 5. Latitudinal and monthly variation of UVI and TOZ percent change in 2090-2100 relative to 2000-2010 for the four RCP scenarios

Atmos. Chem. Phys. Discuss., https://doi.org/10.5194/acp-2018-525
Manuscript under review for journal Atmos. Chem. Phys.
Discussion started: 11 June 2018

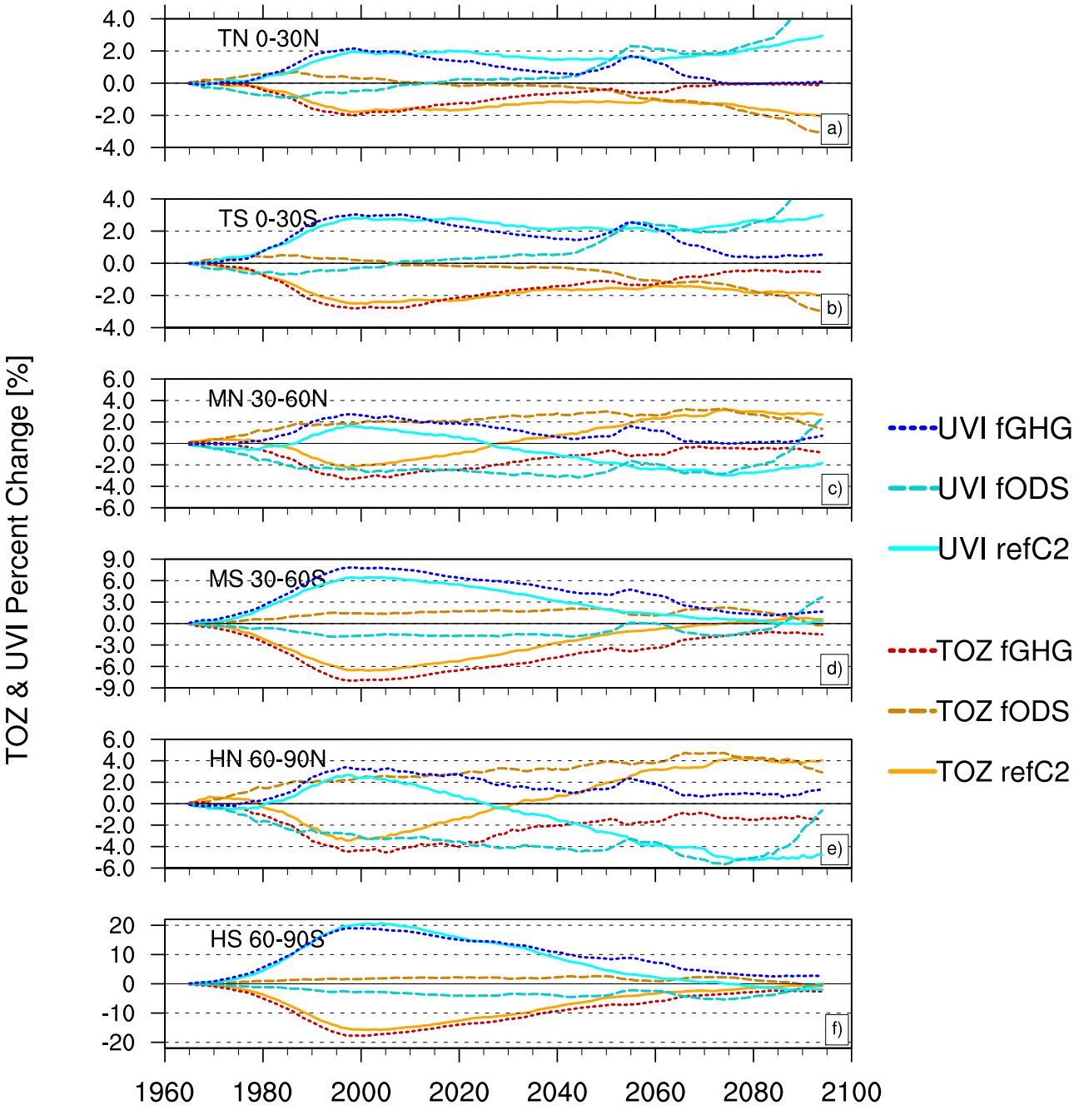

Figure 6. UVI and TOZ percent changes (relative to 1960s values) for six latitudinal bands; Northern Tropical band (0°- 30 °N), Southern Tropical band (0°- 30 °S), Northern Mid Latitude band (30°- 60 °N), Southern Mid Latitude band (30°- 60 °S), Northern High Latitude band (60°- 90 °N), Southern High Latitude band (60°- 90 °S). UVI changes are represented in differents shades of blue for the four RCPs scenarios. TOZ changes are represented in differents shades of red.

Atmos. Chem. Phys. Discuss., https://doi.org/10.5194/acp-2018-525
Manuscript under review for journal Atmos. Chem. Phys.
Discussion started: 11 June 2018

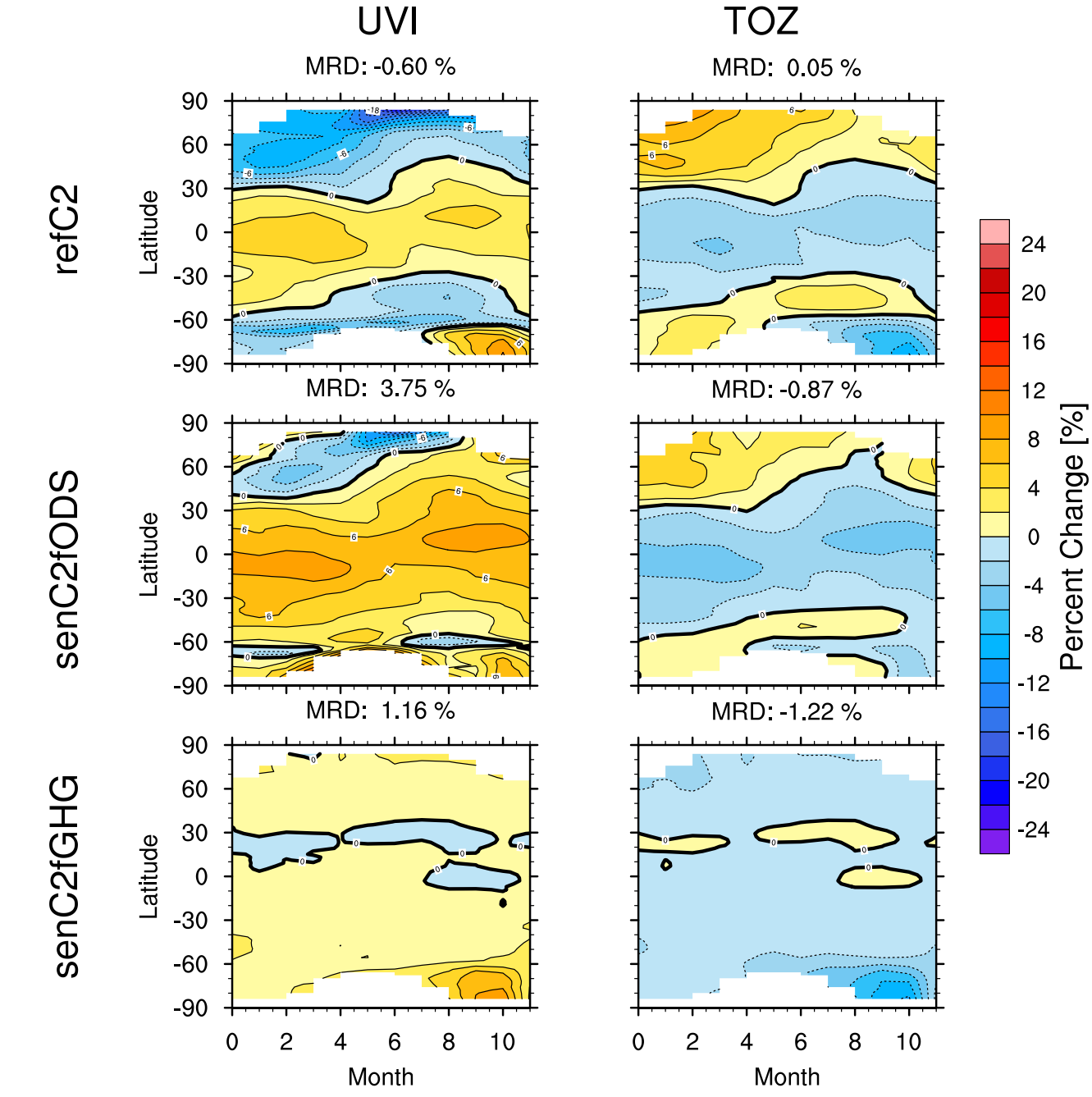

Figure 7. Latitudinal and monthly variation of UVI and TOZ percent change between 2090-2100 and 1960-1970 values for refC2, senC2fODS, senC2fGHG.

Atmos. Chem. Phys. Discuss., https://doi.org/10.5194/acp-2018-525
Manuscript under review for journal Atmos. Chem. Phys.
Discussion started: 11 June 2018

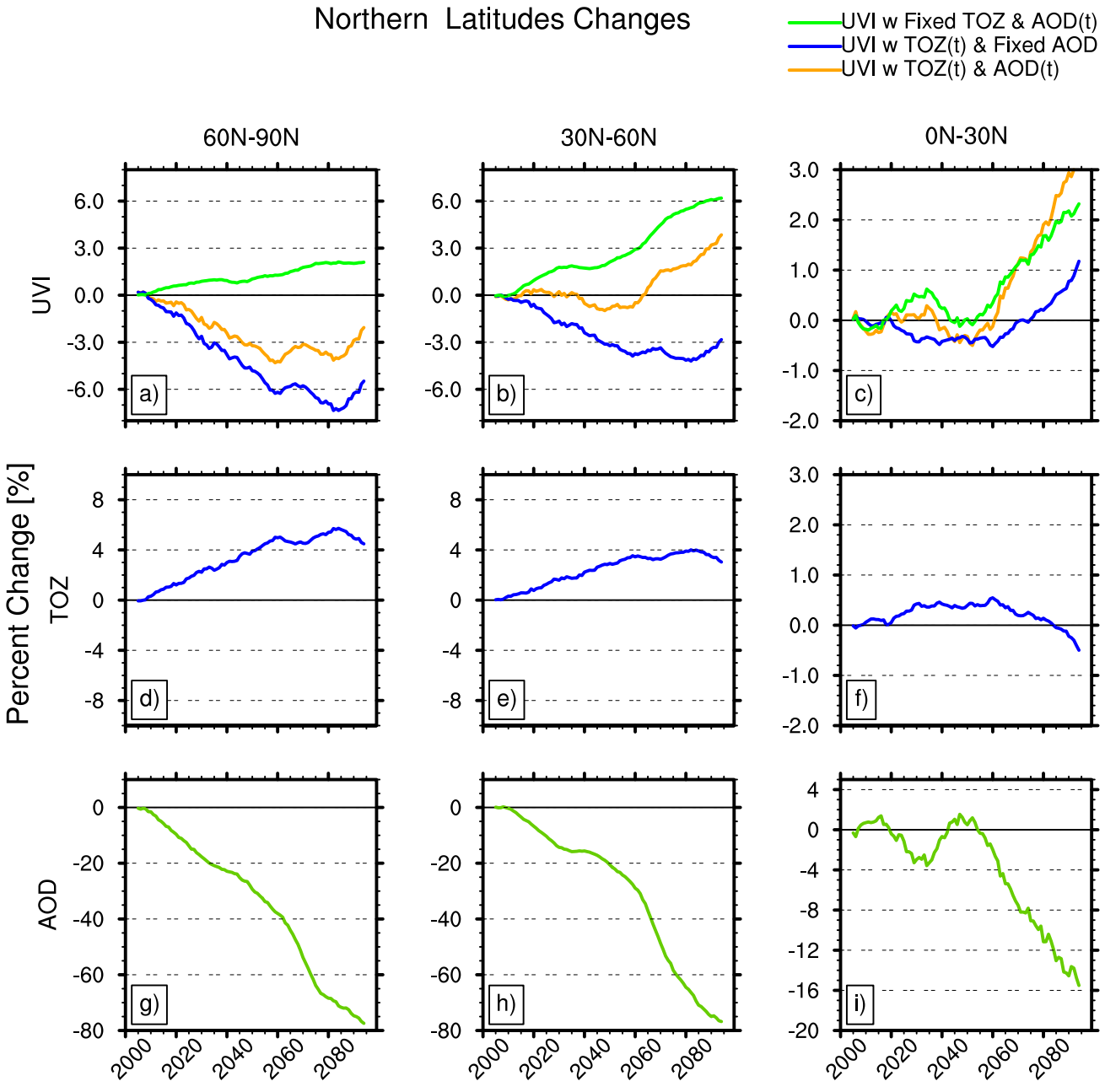

Figure 8. UVI, TOZ and AOD percent change from 2000-2010 values in the northern high, mid, and low latitudes for the EXP3 experiment. UVI modelized with transient TOZ and and AOD fixed at present-day climatological values are in blue. UVI modelized with TOZ fixed at present-day climatological values and AOD variable throught the 21st century are in green. UVI modelized with transient TOZ and AOD are in orange. TOZ and AOD are respectively in blue and green.

Atmos. Chem. Phys. Discuss., https://doi.org/10.5194/acp-2018-525
Manuscript under review for journal Atmos. Chem. Phys.
Discussion started: 11 June 2018

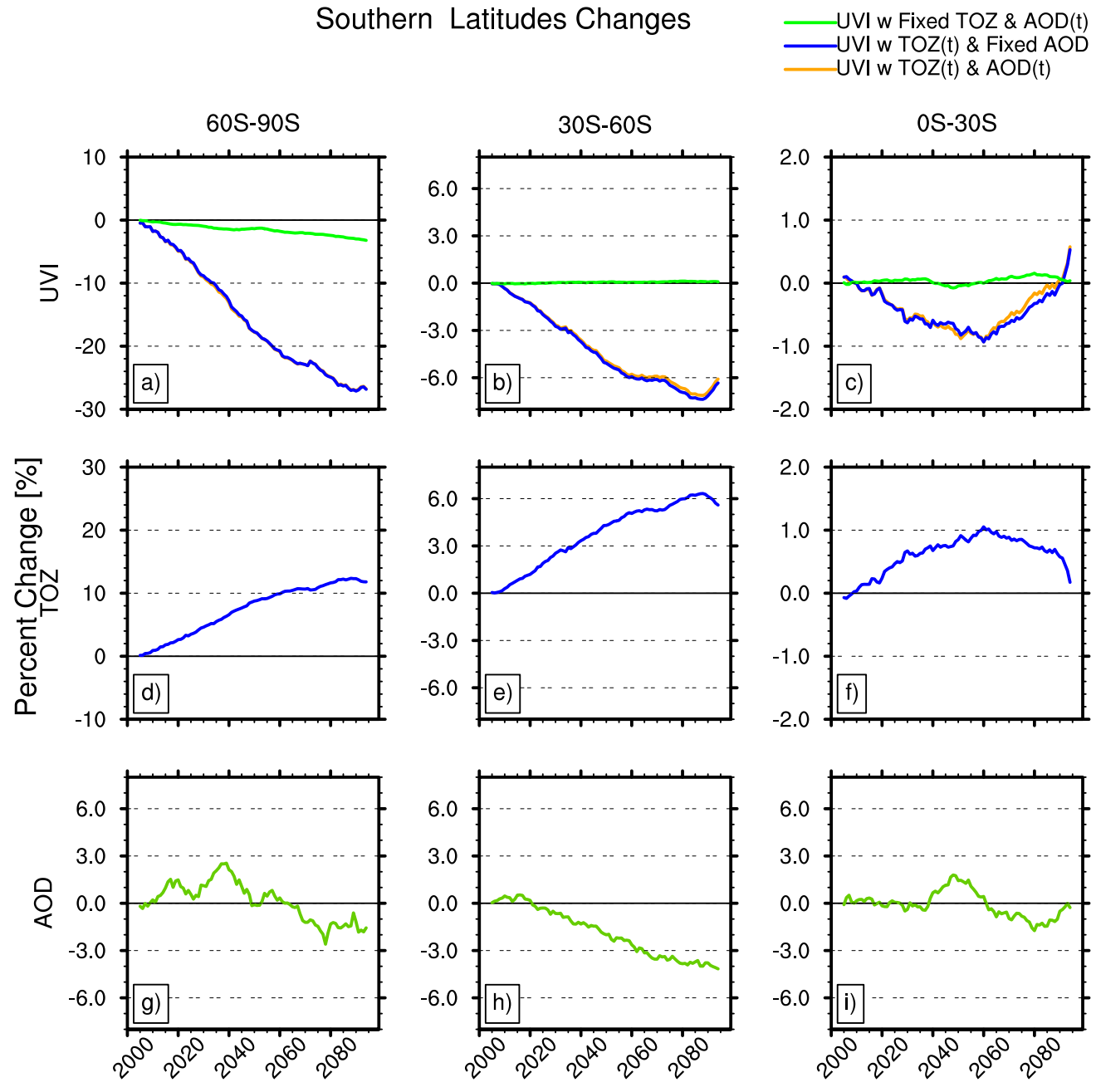

Figure 9. UVI, TOZ and AOD percent change from 2000-2010 values in the southern high, mid, and low latitudes for the EXP3 experiment. UVI calculated with transient TOZ and and AOD fixed at present-day climatological values are in blue. UVI calculated with TOZ fixed at present-day climatological values and AOD variable throught the 21st century are in green. UVI calculated with transient TOZ and AOD are in orange. TOZ and AOD are in blue and green respectively.

Acknowledgements. The authors acknowledge the Région Réunion, CNRS and Université de la Réunion for support and contribution within the research infrastructure OPAR (Observatoire de Physique de l'Atmosphère à la Réunion). OPAR is presently funded by CNRS (INSU) and Université de la Réunion and managed by OSU-R (Observatoires des Sciences de l'Univers à la Réunion, UMS 3365).

The data used in this publication were obtained as part of the Network for the Detection of Atmospheric Composition Change (NDACC) and are publicly available (see http://www.ndacc.org).

We acknowledge the modeling groups for making their simulations available for this analysis, the joint IGBP-IGAC/WCRP-SPARC Chemistry-Climate Model Initiative (CCMI) for organizing and coordinating the model data analysis activity, and the British Atmospheric Data Center (BADC) for collecting and archiving the CCMI model output.

This project was supported by the European Project StratoClim (7th Framework Programme, grant agreement 603557) and the grant "SOLSPEC" from the Centre d'Etude Spatiale (CNES).

The SOCOL team acknowledges support from the Swiss National Science Foundation under grant agreement CRSII2_147659 (FUPSOL II). E.R. acknowledges support from the Swiss National Science Foundation under grants 169241 (VEC) and 163206 (SIMA).

CCSRNIES research was supported by the Environment Research and Technology Development Fund (2-1303 and 2-1709) of the Ministry of the Environment, Japan, and computations were performed on NEC-SX9/A(ECO) computers at the CGER, NIES.

The EMAC simulations have been performed at the German Climate Computing Centre (DKRZ) through support from the Bundesministerium für Bildung und Forschung (BMBF). DKRZ and its scientific steering committee are gratefully acknowledged for providing the HPC and data archiving resources for the consortial project ESCiMo (Earth System Chemistry integrated Modelling).

N.B., and F.M.O'C. were supported by the Joint UK BEIS/Defra Met Office Hadley Centre Climate Programme (GA01101). N.B. also acknowledges the European Commission's 7th Framework Programme, under grant agreement no. 603557, StratoClim project.

Olaf Morgenstern and Guang Zeng wish to acknowledge the contribution of NeSI high-performance computing facilities to the results of this research. New Zealand's national facilities are provided by the New Zealand eScience Infrastructure (NeSI) and funded jointly by NeSI's collaborator institutions and through the Ministry of Business, Innovation & Employment's Research Infrastructure programme (https://www.nesi.org.nz). Olaf Morgenstern acknowledges support from the Royal Society Marsden Fund, grant 12-NIW-006, and under the Deep South National Science Challenge.

References

Akiyoshi, H., Nakamura, T., Miyasaka, T., Shiotani, M., and Suzuki, M.: A nudged chemistry-climate model simulation of chemical constituent distribution at northern high-latitude stratosphere observed by SMILES and MLS during the 2009/2010 stratospheric sudden warming, Journal of Geophysical Research: Atmospheres, 121, 1361–1380, 2016.

Andrews, D. G., Holton, J. R., and Leovy, C. B.: Middle atmosphere dynamics, 40, Academic press, 1987.

Bais, A. F., Zerefos, C. S., Meleti, C., Ziomas, I. C., and Tourpali, K.: Spectral measurements of solar UVB radiation and its relations to total ozone, SO2, and clouds, Journal of Geophysical Research: Atmospheres, 98, 5199–5204, https://doi.org/10.1029/92JD02904, http://dx.doi.org/10.1029/92JD02904, 1993.

Bais, A. F., Tourpali, K., Kazantzidis, A., Akiyoshi, H., Bekki, S., Braesicke, P., Chipperfield, M. P., Dameris, M., Eyring, V., Garny, H., and et al.: Projections of UV radiation changes in the 21st century: impact of ozone recovery and cloud effects, Atmospheric Chemistry and Physics, 11, 7533–7545, https://doi.org/10.5194/acp-11-7533-2011, 2011.

Bednarz, E. M., Maycock, A. C., Abraham, N. L., Braesicke, P., Dessens, O., and Pyle, J. A.: Future Arctic ozone recovery: the importance of chemistry and dynamics, Atmospheric Chemistry and Physics, 16, 12 159–12 176, 2016.

Brewer, A. W.: Evidence for a world circulation provided by the measurements of helium and water vapour distribution in the stratosphere, Quarterly Journal of the Royal Meteorological Society, 75, 351–363, https://doi.org/10.1002/qj.49707532603, http://dx.doi.org/10.1002/qj.49707532603, 1949.

Brogniez, C., Auriol, F., Deroo, C., Arola, A., Kujanpää, J., Sauvage, B., Kalakoski, N., Pitkänen, M. R. A., Catalfamo, M., Metzger, J.-M., and et al.: Validation of satellite-based noontime UVI with NDACC ground-based instruments: influence of topography, environment and satellite overpass time, Atmospheric Chemistry and Physics, 16, 15 049–15 074, https://doi.org/10.5194/acp-16-15049-2016, http://dx.doi.org/10.5194/acp-16-15049-2016, 2016.

Brühl, C. and Crutzen, P. J.: On the disproportionate role of tropospheric ozone as a filter against solar UV-B radiation, Geophysical Research Letters, 16, 703–706, https://doi.org/10.1029/GL016i007p00703, http://dx.doi.org/10.1029/GL016i007p00703, 1989.

Butchart, N.: The Brewer-Dobson circulation, Reviews of Geophysics, 52, 157–184, https://doi.org/10.1002/2013rg000448, 2014.

Butler, A. H., Daniel, J. S., Portmann, R. W., Ravishankara, A. R., Young, P. J., Fahey, D. W., and Rosenlof, K. H.: Diverse policy implications for future ozone and surface UV in a changing climate, Environmental Research Letters, 11, 064 017, http://stacks.iop.org/1748-9326/11/i=6/a=064017, 2016.

Calbó, J., Pagès, D., and González, J.-A.: Empirical studies of cloud effects on UV radiation: A review, Reviews of Geophysics, 43, n/a–n/a, https://doi.org/10.1029/2004RG000155, http://dx.doi.org/10.1029/2004RG000155, rG2002, 2005.

Collins, W. J., Lamarque, J.-F., Schulz, M., Boucher, O., Eyring, V., Hegglin, M. I., Maycock, A., Myhre, G., Prather, M., Shindell, D., and Smith, S. J.: AerChemMIP: quantifying the effects of chemistry and aerosols in CMIP6, Geoscientific Model Development, 10, 585–607, https://doi.org/10.5194/gmd-10-585-2017, https://www.geosci-model-dev.net/10/585/2017/, 2017.

Correa, M. d. P., Godin-Beekmann, S., Haeffelin, M., Bekki, S., Saiag, P., Badosa, J., Jegou, F., Pazmino, A., and Mahe, E.: Projected changes in clear-sky erythemal and vitamin D effective UV doses for Europe over the period 2006 to 2100, Photochem. Photobiol. Sci., 12, 1053–1064, https://doi.org/10.1039/C3PP50024A, 2013.

De Mazière, M., Thompson, A. M., Kurylo, M. J., Wild, J. D., Bernhard, G., Blumenstock, T., Braathen, G. O., Hannigan, J. W., Lambert, J.-C., Leblanc, T., McGee, T. J., Nedoluha, G., Petropavlovskikh, I., Seckmeyer, G., Simon, P. C., Steinbrecht, W., and Strahan, S. E.: The

Network for the Detection of Atmospheric Composition Change (NDACC): history, status and perspectives, Atmospheric Chemistry and Physics, 18, 4935–4964, https://doi.org/10.5194/acp-18-4935-2018, https://www.atmos-chem-phys.net/18/4935/2018/, 2018.

Deushi, M. and Shibata, K.: Development of a Meteorological Research Institute chemistry-climate model version 2 for the study of tropospheric and stratospheric chemistry, Papers in Meteorology and Geophysics, 62, 1–46, 2011.

Dhomse, S., Kinnison, D., Chipperfield, M. P., Cionni, I., Hegglin, M., Abraham, N. L., Akiyoshi, H., Archibald, A. T., Bednarz, E. M., Bekki, S., Braesicke, P., Butchart, N., Dameris, M., Deushi, M., Frith, S., Hardiman, S. C., Hassler, B., Horowitz, L. W., Hu, R.-M., Jöckel, P., Josse, B., Kirner, O., Kremser, S., Langematz, U., Lewis, J., Marchand, M., Lin, M., Mancini, E., Marécal, V., Michou, M., Morgenstern, O., O'Connor, F. M., Oman, L., Pitari, G., Plummer, D. A., Pyle, J. A., Revell, L. E., Rozanov, E., Schofield, R., Stenke, A., Stone, K., Sudo, K., Tilmes, S., Visioni, D., Yamashita, Y., and Zeng, G.: Estimates of Ozone Return Dates from Chemistry-Climate Model Initiative Simulations, Atmospheric Chemistry and Physics Discussions, 2018, 1–40, https://doi.org/10.5194/acp-2018-87, https://www.atmos-chem-phys-discuss.net/acp-2018-87/, 2018.

Dobson, G.: Origin and distribution of the polyatomic molecules in the atmosphere, Proceedings of the Royal Society of London A: Mathematical, Physical and Engineering Sciences, 236, 187–193, https://doi.org/10.1098/rspa.1956.0127, http://rspa.royalsocietypublishing.org/content/236/1205/187, 1956.

Dufresne, J.-L., Foujols, M.-A., Denvil, S., Caubel, A., Marti, O., Aumont, O., Balkanski, Y., Bekki, S., Bellenger, H., Benshila, R., et al.: Climate change projections using the IPSL-CM5 Earth System Model: from CMIP3 to CMIP5, Climate Dynamics, 40, 2123–2165, 2013.

Erickson III, D. J., Sulzberger, B., Zepp, R. G., and Austin, A. T.: Effects of stratospheric ozone depletion, solar UV radiation, and climate change on biogeochemical cycling: interactions and feedbacks, Photochem. Photobiol. Sci., 14, 127–148, https://doi.org/10.1039/C4PP90036G, 2015.

Eyring, V., Lamarque, J.-F., Hess, P., Arfeuille, F., Bowman, K., Chipperfield, M., Duncan, B., Fiore, A., Gettelman, A., Giorgetta, M., Granier, C., Hegglin, M., Kinnison, D., Kunze, M., Langematz, U., Luo, B., Martin, R., Matthes, K., Newman, P., Peter, T., Peter, T., Robock, A., Ryerson, T., Saiz-Lopez, A., Salawitch, R., Schultz, M., Shepherd, T., Shindell, D., Staehelin, J., Tegtmeier, S., Thomason, L., Tilmes, S., Vernier, J.-P., Waugh, D., and Young, P.: Overview of IGAC/SPARC Chemistry-Climate Model Initiative (CCMI) Community Simulations in Support of Upcoming Ozone and Climate Assessments, eyring et al. (2013), Overview of IGAC/SPARC Chemistry-Climate Model Initiative (CCMI) Community Simulations in Support of Upcoming Ozone and Climate Assessments, SPARC Newsletter no. 40, WMO-WRCP, Geneva, Switzerland, 48-66., 2013.

Fleming, E. L., Jackman, C. H., Stolarski, R. S., and Douglass, A. R.: A model study of the impact of source gas changes on the stratosphere for 1850–2100, Atmospheric Chemistry and Physics, 11, 8515–8541, https://doi.org/10.5194/acp-11-8515-2011, https://www.atmos-chem-phys.net/11/8515/2011/, 2011.

Frederick, J. E., Snell, H. E., and Haywood, E. K.: SOLAR ULTRAVIOLET RADIATION AT THE EARTH'S SURFACE, Photochemistry and Photobiology, 50, 443–450, https://doi.org/10.1111/j.1751-1097.1989.tb05548.x, http://dx.doi.org/10.1111/j.1751-1097.1989.tb05548.x, 1989.

Garcia, R. R., Smith, A. K., Kinnison, D. E., Cámara, Á. d. l., and Murphy, D. J.: Modification of the gravity wave parameterization in the Whole Atmosphere Community Climate Model: Motivation and results, Journal of the Atmospheric Sciences, 74, 275–291, 2017.

Gorshelev, V., Serdyuchenko, A., Weber, M., Chehade, W., and Burrows, J. P.: High spectral resolution ozone absorption cross-sections – Part 1: Measurements, data analysis and comparison with previous measurements around 293 K, Atmospheric Measurement Techniques, 7, 609–624, https://doi.org/10.5194/amt-7-609-2014, 2014.

Gray, L. J., Beer, J., Geller, M., Haigh, J. D., Lockwood, M., Matthes, K., Cubasch, U., Fleitmann, D., Harrison, G., Hood, L., et al.: Solar influences on climate, Reviews of Geophysics, 48, 2010.

Guth, J., Josse, B., Marécal, V., Joly, M., and Hamer, P.: First implementation of secondary inorganic aerosols in the MOCAGE version R2. 15.0 chemistry transport model, Geoscientific Model Development, 9, 137, 2016.

Hader, D.-P., Kumar, H. D., Smith, R. C., and Worrest, R. C.: Effects of solar UV radiation on aquatic ecosystems and interactions with climate change, Photochem. Photobiol. Sci., 6, 267–285, https://doi.org/10.1039/B700020K, 2007.

Hardiman, S. C., Butchart, N., O'Connor, F. M., and Rumbold, S. T.: The Met Office HadGEM3-ES chemistry-climate model: evaluation of stratospheric dynamics and its impact on ozone, Geoscientific Model Development, 10, 1209, 2017.

Hegglin, M. and Lamarque, J.: The IGAC/SPARC Chemistry-Climate Model Initiative Phase-1 (CCMI-1) model data output, NCAS British Atmospheric Data Centre http://catalogue. ceda. ac. uk/uuid/9cc6b94df0f4469d8066d69b5df879d5, 2015.

Hegglin, M. I. and Shepherd, T. G.: Large climate-induced changes in ultraviolet index and stratosphere-to-troposphere ozone flux, Nature Geoscience, 2, 687–691, https://doi.org/10.1038/ngeo604, 2009.

Holick, M. F., MacLaughlin, J., Clark, M., Holick, S., Potts, J., Anderson, R., Blank, I., Parrish, J., and Elias, P.: Photosynthesis of previtamin D3 in human skin and the physiologic consequences, Science, 210, 203–205, 1980.

Holton, J. R., Haynes, P. H., McIntyre, M. E., Douglass, A. R., Rood, R. B., and Pfister, L.: Stratosphere-troposphere exchange, Reviews of Geophysics, 33, 403–439, https://doi.org/10.1029/95RG02097, http://dx.doi.org/10.1029/95RG02097, 1995.

Hunke, E. C., Lipscomb, W. H., Turner, A. K., Jeffery, N., and Elliott, S.: CICE: the Los Alamos Sea Ice Model Documentation and Software User's Manual Version 4.1 LA-CC-06-012, T-3 Fluid Dynamics Group, Los Alamos National Laboratory, 675, 2010.

Imai, K., Manago, N., Mitsuda, C., Naito, Y., Nishimoto, E., Sakazaki, T., Fujiwara, M., Froidevaux, L., Clarmann, T., Stiller, G. P., et al.: Validation of ozone data from the Superconducting Submillimeter-Wave Limb-Emission Sounder (SMILES), Journal of Geophysical Research: Atmospheres, 118, 5750–5769, 2013.

IPCC: Climate Change 2013: The Physical Science Basis. Contribution of Working Group I to the Fifth Assessment Report of the Intergovernmental Panel on Climate Change, Cambridge University Press, Cambridge, United Kingdom and New York, NY, USA, https://doi.org/10.1017/CBO9781107415324, www.climatechange2013.org, 2013.

Jégou, F., Godin-Beekmann, S., Corrêa, M., Brogniez, C., Auriol, F., Peuch, V., Haeffelin, M., Pazmino, A., Saiag, P., Goutail, F., et al.: Validity of satellite measurements used for the monitoring of UV radiation risk on health, Atmospheric Chemistry and Physics, 11, 13 377–13 394, 2011.

Jöckel, P., Kerkweg, A., Pozzer, A., Sander, R., Tost, H., Riede, H., Baumgaertner, A., Gromov, S., and Kern, B.: Development cycle 2 of the modular earth submodel system (MESSy2), Geoscientific Model Development, 3, 717, 2010.

Jöckel, P., Tost, H., Pozzer, A., Kunze, M., Kirner, O., Brenninkmeijer, C. A. M., Brinkop, S., Cai, D. S., Dyroff, C., Eckstein, J., Frank, F., Garny, H., Gottschaldt, K.-D., Graf, P., Grewe, V., Kerkweg, A., Kern, B., Matthes, S., Mertens, M., Meul, S., Neumaier, M., Nützel, M., Oberländer-Hayn, S., Ruhnke, R., Runde, T., Sander, R., Scharffe, D., and Zahn, A.: Earth System Chemistry integrated Modelling (ESCiMo) with the Modular Earth Submodel System (MESSy) version 2.51, Geoscientific Model Development, 9, 1153–1200, https://doi.org/10.5194/gmd-9-1153-2016, https://www.geosci-model-dev.net/9/1153/2016/, 2016.

Jonsson, A., De Grandpre, J., Fomichev, V., McConnell, J., and Beagley, S.: Doubled CO2-induced cooling in the middle atmosphere: Photochemical analysis of the ozone radiative feedback, Journal of Geophysical Research: Atmospheres, 109, 2004.

Josse, B., Simon, P., and Peuch, V.-H.: Radon global simulations with the multiscale chemistry and transport model MOCAGE, Tellus B, 56, 339–356, 2004.

Kazadzis, S., Kouremeti, N., Bais, A., Kazantzidis, A., and Meleti, C.: Aerosol forcing efficiency in the UVA region from spectral solar irradiance measurements at an urban environment, Annales Geophysicae, 27, 2515–2522, https://doi.org/10.5194/angeo-27-2515-2009, https://www.ann-geophys.net/27/2515/2009/, 2009.

Kinne, S., O'Donnel, D., Stier, P., Kloster, S., Zhang, K., Schmidt, H., Rast, S., Giorgetta, M., Eck, T. F., and Stevens, B.: MAC-v1: A new global aerosol climatology for climate studies, Journal of Advances in Modeling Earth Systems, 5, 704–740, https://doi.org/10.1002/jame.20035, http://dx.doi.org/10.1002/jame.20035, 2013.

Kirner, O., Ruhnke, R., and Sinnhuber, B.-M.: Chemistry–Climate Interactions of Stratospheric and Mesospheric Ozone in EMAC Long-Term Simulations with Different Boundary Conditions for CO2, CH4, N2O, and ODS, Atmosphere-Ocean, 53, 140–152, https://doi.org/10.1080/07055900.2014.980718, 2015.

Koepke, P., Bais, A., Balis, D., Buchwitz, M., Backer, H., Cabo, X., Eckert, P., Eriksen, P., Gillotay, D., Heikkilä, A., et al.: Comparison of models used for UV index calculations, Photochemistry and Photobiology, 67, 657–662, 1998.

Krotkov, N. A., Herman, J., Bhartia, P. K., Seftor, C., Arola, A., Kaurola, J., Taalas, P., and Vasilkov, A.: OMI Surface UV Irradi- ance Algorithm, in OMI Algorithm Theoretical Basis Document, Volume III: Clouds, Aerosols, and Surface UV Irradiance, ATBD-OMI-03, 2002.

Krzyścin, J. W. and Puchalski, S.: Aerosol impact on the surface UV radiation from the ground-based measurements taken at Belsk, Poland, 1980–1996, Journal of Geophysical Research: Atmospheres, 103, 16 175–16 181, https://doi.org/10.1029/98JD00899, http://dx.doi.org/10.1029/98JD00899, 1998.

Lamy, K., Portafaix, T., Brogniez, C., Godin-Beekmann, S., Bencherif, H., Morel, B., Pazmino, A., Metzger, J. M., Auriol, F., Deroo, C., Duflot, V., Goloub, P., and Long, C. N.: Ultraviolet radiation modelling from ground-based and satellite measurements on Reunion Island, southern tropics, Atmospheric Chemistry and Physics, 18, 227–246, https://doi.org/10.5194/acp-18-227-2018, https://www.atmos-chem-phys.net/18/227/2018/, 2018.

Madec, G. et al.: NEMO ocean engine, 2015.

Madronich, S.: Analytic Formula for the Clear sky UV Index, Photochemistry and Photobiology, 83, 1537–1538, https://doi.org/10.1111/j.1751-1097.2007.00200.x, 2007.

Madronich, S., McKenzie, R. L., Björn, L. O., and Caldwell, M. M.: Changes in biologically active ultraviolet radiation reaching the Earth's surface, Journal of Photochemistry and Photobiology B: Biology, 46, 5 – 19, 1998.

Marchand, M., Keckhut, P., Lefebvre, S., Claud, C., Cugnet, D., Hauchecorne, A., Lefèvre, F., Lefebvre, M.-P., Jumelet, J., Lott, F., et al.: Dynamical amplification of the stratospheric solar response simulated with the Chemistry-Climate model LMDz-Reprobus, Journal of Atmospheric and Solar-Terrestrial Physics, 75, 147–160, 2012.

Marsh, D. R., Mills, M. J., Kinnison, D. E., Lamarque, J.-F., Calvo, N., and Polvani, L. M.: Climate change from 1850 to 2005 simulated in CESM1 (WACCM), Journal of climate, 26, 7372–7391, 2013.

Masui, T., Matsumoto, K., Hijioka, Y., Kinoshita, T., Nozawa, T., Ishiwatari, S., Kato, E., Shukla, P. R., Yamagata, Y., and Kainuma, M.: An emission pathway for stabilization at 6 Wm2 radiative forcing, Climatic Change, 109, 59, https://doi.org/10.1007/s10584-011-0150-5, 2011.

Matsumura, Y. and Ananthaswamy, H. N.: Toxic effects of ultraviolet radiation on the skin, Toxicology and applied pharmacology, 195, 298–308, 2004.

Mayer, B., Kylling, A., Madronich, S., and Seckmeyer, G.: Enhanced absorption of UV radiation due to multiple scattering in clouds: Experimental evidence and theoretical explanation, Journal of Geophysical Research: Atmospheres, 103, 31 241–31 254, https://doi.org/10.1029/98JD02676, http://dx.doi.org/10.1029/98JD02676, 1998.

Mc Kinlay, A. F. and Diffey, B. L.: A reference action spectrum for ultraviolet induced erythema in human skin, CIE J, 6, 17–22, 1987.

Meftah, M., Bolsée, D., Damé, L., Hauchecorne, A., Pereira, N., Irbah, A., Bekki, S., Cessateur, G., Foujols, T., and Thiéblemont, R.: Solar Irradiance from 165 to 400 nm in 2008 and UV Variations in Three Spectral Bands During Solar Cycle 24, Solar Physics, 291, 3527–3547, https://doi.org/10.1007/s11207-016-0997-8, https://doi.org/10.1007/s11207-016-0997-8, 2016.

Meinshausen, M., Smith, S. J., Calvin, K., Daniel, J. S., Kainuma, M. L. T., Lamarque, J.-F., Matsumoto, K., Montzka, S. A., Raper, S. C. B., Riahi, K., Thomson, A., Velders, G. J. M., and van Vuuren, D. P.: The RCP greenhouse gas concentrations and their extensions from 1765 to 2300, Climatic Change, 109, 213, https://doi.org/10.1007/s10584-011-0156-z, 2011.

Michou, M., Saint-Martin, D., Teyssedre, H., Alias, A., Karcher, F., Olivié, D., Voldoire, A., Josse, B., Peuch, V.-H., Clark, H., et al.: A new version of the CNRM Chemistry-Climate Model, CNRM-CCM: description and improvements from the CCMVal-2 simulations, Geoscientific Model Development, 4, 873–900, 2011.

Molod, A., Takacs, L., Suarez, M., and Bacmeister, J.: Development of the GEOS-5 atmospheric general circulation model: Evolution from MERRA to MERRA2, Geoscientific Model Development, 8, 1339, 2015.

Morgenstern, O., Braesicke, P., Hurwitz, M. M., O'Connor, F. M., Bushell, A. C., Johnson, C. E., and Pyle, J. A.: The World Avoided by the Montreal Protocol, Geophysical Research Letters, 35, n/a–n/a, https://doi.org/10.1029/2008GL034590, http://dx.doi.org/10.1029/2008GL034590, l16811, 2008.

Morgenstern, O., Braesicke, P., O'Connor, F. M., Bushell, A. C., Johnson, C. E., Osprey, S. M., and Pyle, J. A.: Evaluation of the new UKCA climate-composition model – Part 1: The stratosphere, Geoscientific Model Development, 2, 43–57, https://doi.org/10.5194/gmd-2-43-2009, https://www.geosci-model-dev.net/2/43/2009/, 2009.

Morgenstern, O., Hegglin, M. I., Rozanov, E., O'Connor, F. M., Abraham, N. L., Akiyoshi, H., Archibald, A. T., Bekki, S., Butchart, N., Chipperfield, M. P., Deushi, M., Dhomse, S. S., Garcia, R. R., Hardiman, S. C., Horowitz, L. W., Jöckel, P., Josse, B., Kinnison, D., Lin, M., Mancini, E., Manyin, M. E., Marchand, M., Marécal, V., Michou, M., Oman, L. D., Pitari, G., Plummer, D. A., Revell, L. E., Saint-Martin, D., Schofield, R., Stenke, A., Stone, K., Sudo, K., Tanaka, T. Y., Tilmes, S., Yamashita, Y., Yoshida, K., and Zeng, G.: Review of the global models used within phase 1 of the Chemistry–Climate Model Initiative (CCMI), Geoscientific Model Development, 10, 639–671, https://doi.org/10.5194/gmd-10-639-2017, https://www.geosci-model-dev.net/10/639/2017/, 2017.

Morgenstern, O., Stone, K. A., Schofield, R., Akiyoshi, H., Yamashita, Y., Kinnison, D. E., Garcia, R. R., Sudo, K., Plummer, D. A., Scinocca, J., Oman, L. D., Manyin, M. E., Zeng, G., Rozanov, E., Stenke, A., Revell, L. E., Pitari, G., Mancini, E., Di Genova, G., Visioni, D., Dhomse, S. S., and Chipperfield, M. P.: Ozone sensitivity to varying greenhouse gases and ozone-depleting substances in CCMI-1 simulations, Atmospheric Chemistry and Physics, 18, 1091–1114, https://doi.org/10.5194/acp-18-1091-2018, https://www.atmos-chem-phys.net/18/1091/2018/, 2018.

O'Connor, F., Johnson, C., Morgenstern, O., Abraham, N., Braesicke, P., Dalvi, M., Folberth, G., Sanderson, M., Telford, P., Voulgarakis, A., et al.: Evaluation of the new UKCA climate-composition model–Part 2: The Troposphere, Geoscientific Model Development, 7, 41–91, 2014.

Oman, L., Ziemke, J., Douglass, A., Waugh, D., Lang, C., Rodriguez, J., and Nielsen, J.: The response of tropical tropospheric ozone to ENSO, Geophysical Research Letters, 38, 2011.

Pitari, G., Aquila, V., Kravitz, B., Robock, A., Watanabe, S., Cionni, I., Luca, N. D., Genova, G. D., Mancini, E., and Tilmes, S.: Stratospheric ozone response to sulfate geoengineering: Results from the Geoengineering Model Intercomparison Project (GeoMIP), Journal of Geophysical Research: Atmospheres, 119, 2629–2653, 2014.

Poulain, V., Bekki, S., Marchand, M., Chipperfield, M., Khodri, M., Lefèvre, F., Dhomse, S., Bodeker, G., Toumi, R., Maziere, M. D., Pommereau, J.-P., Pazmino, A., Goutail, F., Plummer, D., Rozanov, E., Mancini, E., Akiyoshi, H., Lamarque, J.-F., and Austin, J.: Evaluation of the inter-annual variability of stratospheric chemical composition in chemistry-climate models using ground-based multi species time series, Journal of Atmospheric and Solar-Terrestrial Physics, 145, 61 – 84, https://doi.org/https://doi.org/10.1016/j.jastp.2016.03.010, http://www.sciencedirect.com/science/article/pii/S136468261630092X, 2016.

Revell, L., Tummon, F., Stenke, A., Sukhodolov, T., Coulon, A., Rozanov, E., Garny, H., Grewe, V., and Peter, T.: Drivers of the tropospheric ozone budget throughout the 21st century under the medium-high climate scenario RCP 6.0, Atmospheric Chemistry and Physics, 15, 5887–5902, 2015.

Revell, L. E., Bodeker, G. E., Huck, P. E., Williamson, B. E., and Rozanov, E.: The sensitivity of stratospheric ozone changes through the 21st century to N_2O and CH_4, Atmospheric Chemistry and Physics, 12, 11 309–11 317, https://doi.org/10.5194/acp-12-11309-2012, https://www.atmos-chem-phys.net/12/11309/2012/, 2012.

Rind, D., Suozzo, R., Balachandran, N. K., and Prather, M. J.: Climate Change and the Middle Atmosphere. Part I: The Doubled CO2 Climate, Journal of the Atmospheric Sciences, 47, 475–494, https://doi.org/10.1175/1520-0469(1990)047<0475:CCATMA>2.0.CO;2, 1990.

Rind, D., Lerner, J., Prather, M., and McLinden, C.: Stratospheric Circulation and Tracer/Ozone Changes in Response to Alternative Doubled CO2 Climate Depictions, in: AGU Fall Meeting Abstracts, 2001.

Scinocca, J., McFarlane, N., Lazare, M., Li, J., and Plummer, D.: The CCCma third generation AGCM and its extension into the middle atmosphere, Atmospheric Chemistry and Physics, 8, 7055–7074, 2008.

Sekiya, T. and Sudo, K.: Role of meteorological variability in global tropospheric ozone during 1970–2008, Journal of Geophysical Research: Atmospheres, 117, 2012.

Serdyuchenko, A., Gorshelev, V., Weber, M., Chehade, W., and Burrows, J.: High spectral resolution ozone absorption cross-sections–Part 2: Temperature dependence., Atmospheric Measurement Techniques Discussions, 6, 2014.

Shepherd, T. G.: Dynamics, stratospheric ozone, and climate change, Atmosphere-Ocean, 46, 117–138, https://doi.org/10.3137/ao.460106, 2008.

Smith, R. C. and Cullen, J. J.: Effects of UV radiation on phytoplankton, Reviews of Geophysics, 33, 1211–1223, https://doi.org/10.1029/95RG00801, http://dx.doi.org/10.1029/95RG00801, 1995.

Solomon, S., Portmann, R., Sanders, R., Daniel, J., Madsen, W., Bartram, B., and Dutton, E.: On the role of nitrogen dioxide in the absorption of solar radiation, Journal of Geophysical Research: Atmospheres, 104, 12 047–12 058, 1999.

Solomon, S., Kinnison, D., Bandoro, J., and Garcia, R.: Simulation of polar ozone depletion: An update, Journal of Geophysical Research: Atmospheres, 120, 7958–7974, 2015.

Solomon, S., Ivy, D. J., Kinnison, D., Mills, M. J., Neely, R. R., and Schmidt, A.: Emergence of healing in the Antarctic ozone layer, Science, https://doi.org/10.1126/science.aae0061, 2016.

Stenke, A., Schraner, M., Rozanov, E., Egorova, T., Luo, B., and Peter, T.: The SOCOL version 3.0 chemistry–climate model: description, evaluation, and implications from an advanced transport algorithm, Geoscientific Model Development, 6, 1407–1427, 2013.

Stone, K. A., Morgenstern, O., Karoly, D. J., Klekociuk, A. R., French, W. J., Abraham, N. L., and Schofield, R.: Evaluation of the ACCESS – chemistry–climate model for the Southern Hemisphere, Atmospheric Chemistry and Physics, 16, 2401–2415, https://doi.org/10.5194/acp-16-2401-2016, https://www.atmos-chem-phys.net/16/2401/2016/, 2016.

Sudo, K., Takahashi, M., Kurokawa, J.-i., and Akimoto, H.: CHASER: A global chemical model of the troposphere 1. Model description, Journal of Geophysical Research: Atmospheres, 107, 2002.

Szopa, S., Balkanski, Y., Schulz, M., Bekki, S., Cugnet, D., Fortems-Cheiney, A., Turquety, S., Cozic, A., Déandreis, C., Hauglustaine, D., et al.: Aerosol and ozone changes as forcing for climate evolution between 1850 and 2100, Climate dynamics, 40, 2223–2250, 2013.

Takemura, T.: Distributions and climate effects of atmospheric aerosols from the preindustrial era to 2100 along Representative Concentration Pathways (RCPs) simulated using the global aerosol model SPRINTARS, Atmospheric Chemistry and Physics, 12, 11 555–11 572, https://doi.org/10.5194/acp-12-11555-2012, https://www.atmos-chem-phys.net/12/11555/2012/, 2012.

Tanskanen, A., Lindfors, A., Määttä, A., Krotkov, N., Herman, J., Kaurola, J., Koskela, T., Lakkala, K., Fioletov, V., Bernhard, G., and et al.: Validation of daily erythemal doses from Ozone Monitoring Instrument with ground-based UV measurement data, Journal of Geophysical Research, 112, https://doi.org/10.1029/2007jd008830, http://dx.doi.org/10.1029/2007JD008830, 2007.

Tian, W. and Chipperfield, M. P.: A new coupled chemistry–climate model for the stratosphere: The importance of coupling for future O3-climate predictions, Quarterly Journal of the Royal Meteorological Society, 131, 281–303, 2005.

Vaida, V., Kjaergaard, H. G., Hintze, P. E., and Donaldson, D. J.: Photolysis of Sulfuric Acid Vapor by Visible Solar Radiation, Science, 299, 1566–1568, https://doi.org/10.1126/science.1079297, http://science.sciencemag.org/content/299/5612/1566, 2003.

van Vuuren, D. P., Edmonds, J., Kainuma, M., Riahi, K., Thomson, A., Hibbard, K., Hurtt, G. C., Kram, T., Krey, V., Lamarque, J.-F., Masui, T., Meinshausen, M., Nakicenovic, N., Smith, S. J., and Rose, S. K.: The representative concentration pathways: an overview, Climatic Change, 109, 5, https://doi.org/10.1007/s10584-011-0148-z, https://doi.org/10.1007/s10584-011-0148-z, 2011.

Voldoire, A., Sanchez-Gomez, E., y Mélia, D. S., Decharme, B., Cassou, C., Sénési, S., Valcke, S., Beau, I., Alias, A., Chevallier, M., et al.: The CNRM-CM5. 1 global climate model: description and basic evaluation, Climate Dynamics, 40, 2091–2121, 2013.

Walters, D., Williams, K., Boutle, I., Bushell, A., Edwards, J., Field, P., Lock, A., Morcrette, C., Stratton, R., Wilkinson, J., et al.: The Met Office unified model global atmosphere 4.0 and JULES global land 4.0 configurations, Geoscientific Model Development, 7, 361–386, 2014.

Watanabe, S., Hajima, T., Sudo, K., Nagashima, T., Takemura, T., Okajima, H., Nozawa, T., Kawase, H., Abe, M., Yokohata, T., et al.: MIROC-ESM 2010: Model description and basic results of CMIP5-20c3m experiments, Geoscientific Model Development, 4, 845, 2011.

WMO, W. M. O.: Scientific assessment of ozone depletion: 2014, Global Ozone Research and Monitoring Project-Report No. 55, 2011.

WMO, W. M. O.: Scientific Assessment of Ozone Depletion: 2014, in: Scientific Assessment of Ozone Depletion: 2014, 55, p. 416, Geneva, Switzerland, 2014.

Yukimoto, S., Adachi, Y., Hosaka, M., Sakami, T., Yoshimura, H., Hirabara, M., Tanaka, T. Y., Shindo, E., Tsujino, H., Deushi, M., et al.: A new global climate model of the Meteorological Research Institute: MRI-CGCM3—model description and basic performance—, Journal of the Meteorological Society of Japan. Ser. II, 90, 23–64, 2012.

Zepp, R. G., Erickson III, D. J., Paul, N. D., and Sulzberger, B.: Interactive effects of solar UV radiation and climate change on biogeochemical cycling, Photochem. Photobiol. Sci., 6, 286–300, https://doi.org/10.1039/B700021A, http://dx.doi.org/10.1039/B700021A, 2007.

Zerefos, C., Mantis, H., Bais, A., Ziomas, I., and Zoumakis, N.: Solar ultraviolet absorption by sulphur dioxide in Thessaloniki, Greece, Atmosphere-Ocean, 24, 292–300, 1986.